Neurobiology of Disease

p75^{NTR} and Its Ligand ProNGF Activate Paracrine Mechanisms Etiological to the Vascular, Inflammatory, and Neurodegenerative Pathologies of Diabetic Retinopathy

Pablo F. Barcelona,[1,2]* Nicholas Sitaras,[3]* Alba Galan,[1] Gema Esquiva,[4] Sean Jmaeff,[1,2] Yifan Jian,[5] Marinko V. Sarunic,[5] Nicolas Cuenca,[4] Przemyslaw Sapieha,[3,6,7]* and H. Uri Saragovi[1,2,8]*

[1]Lady Davis Institute-Jewish General Hospital, Center for Translational Research, McGill University, Montreal, Quebec H3T 1E2, Canada, [2]Department of Pharmacology and Therapeutics, McGill University, Montreal, Quebec H3G 1Y6, Canada, [3]Department of Ophthalmology, Maisonneuve-Rosemont Hospital Research Centre, University of Montreal, Montreal, Quebec H1T 2M4, Canada, [4]Department of Physiology, Genetics and Microbiology, University of Alicante, Alicante CP 03690, Spain, [5]School of Engineering Science, Simon Fraser University, Burnaby, British Columbia V5A 1S6, Canada, [6]Department of Biochemistry, Maisonneuve-Rosemont Hospital Research Centre, University of Montreal, Montreal, Quebec H1T 2M4, Canada, [7]Department of Neurology-Neurosurgery, McGill University, Montreal, Quebec H3A 2B4, Canada, and [8]McGill Cancer Center, McGill University, Montreal, Quebec H3A 1A3, Canada

In many diseases, expression and ligand-dependent activity of the p75^{NTR} receptor can promote pericyte and vascular dysfunction, inflammation, glial activation, and neurodegeneration. Diabetic retinopathy (DR) is characterized by all of these pathological events. However, the mechanisms by which p75^{NTR} may be implicated at each stage of DR pathology remain poorly understood. Using a streptozotocin mouse model of diabetic retinopathy, we report that p75^{NTR} is upregulated very early in glia and in pericytes to mediate ligand-dependent induction of inflammatory cytokines, disruption of the neuro-glia-vascular unit, promotion of blood–retina barrier breakdown, edema, and neuronal death. In a mouse model of oxygen-induced retinopathy, mimicking proliferative DR, p75^{NTR}-dependent inflammation leads to ischemia and pathological angiogenesis through Semaphorin 3A. The acute use of antagonists of p75^{NTR} or antagonists of the ligand proNGF suppresses each distinct phase of pathology, ameliorate disease, and prevent disease progression. Thus, our study documents novel disease mechanisms and validates druggable targets for diabetic retinopathy.

Key words: **diabetes; neurodegeneration; neurotrophin; pathophysiology; receptor; retina**

Significance Statement

Diabetic retinopathy (DR) affects an estimated 250 million people and has no effective treatment. Stages of progression comprise pericyte/vascular dysfunction, inflammation, glial activation, and neurodegeneration. The pathophysiology of each stage remains unclear. We postulated that the activity of p75NTR may be implicated. We show that p75NTR in glia and in pericytes mediate ligand-dependent induction of inflammatory cytokines, disruption of the neuro-glia-vascular unit, promotion of blood–retina barrier breakdown, edema, and neuronal death. p75NTR-promoted inflammation leads to ischemia and angiogenesis through Semaphorin 3A. Antagonists of p75NTR or antagonists of proNGF suppress each distinct phase of pathology, ameliorate disease, and prevent disease progression. Our study documents novel mechanisms in a pervasive disease and validates druggable targets for treatment.

Introduction

Diabetic retinopathy (DR) is a major cause of reduced vision in the working age population (Yau et al., 2012) and leads to irreversible vision loss in ~75% of patients (Heng et al., 2013). DR is a retinal disorder that is characterized by several distinct phases, such as loss of the blood–retina barrier (BRB) function and capillary loss leading to diabetic macular edema (DME). DME is characterized by extravasation of fluids from retinal circulation

Received Nov. 26, 2015; revised June 10, 2016; accepted July 5, 2016.

Author contributions: P.F.B., N.C., P.S., and H.U.S. designed research; P.F.B., N.S., A.G., G.E., and S.J. performed research; Y.J. and M.V.S. contributed unpublished reagents/analytic tools; P.F.B., N.S., A.G., G.E., S.J., Y.J., M.V.S., N.C., P.S., and H.U.S. analyzed data; P.F.B., N.S., P.S., and H.U.S. wrote the paper.

This work was supported by the Canadian Institutes of Health Research and the Foundation to Fight Blindness to H.U.S. and the Canadian Diabetes Association to P.S.

McGill University has patents applied or issued (H.U.S., inventor) covering the compounds used herein. The remaining authors declare no competing financial interests.

*P.F.B. and N.S. contributed equally to this study as first coauthors. H.U.S. and P.S. shared senior authorship to this study.

Correspondence should be addressed to Dr. H. Uri Saragovi, McGill University, 3755 Cote St. Catherine, E-535, Montreal, Quebec H3T 1E2, Canada. E-mail: uri.saragovi@mcgill.ca.

DOI:10.1523/JNEUROSCI.4278-15.2016

 0270-6474/16/368826-16$15.00/0

into the retina, which can lead to significant decreases in visual acuity (Antonetti et al., 2012; Yau et al., 2012). Later stages are associated with retinal ischemia causing hypoxia and a subsequent phase of VEGF-mediated neovessel growth or proliferative DR (PDR). Preventing destructive angiogenesis remains the only current treatment modality for PDR (Antonetti et al., 2012; Heng et al., 2013).

Accumulating evidence points to defects of the neurovascular unit (neurons, glia, and vessels) (Binet et al., 2013; Cerani et al., 2013; Joyal et al., 2013; Dejda et al., 2014) throughout the progression of DR and during pathological preretinal neovascularization (NV), suggesting that the pathophysiology of DR is not purely vascular in nature (Abcouwer and Gardner, 2014). For instance, retinal oxidative stress resulting from hyperglycemia and hyperlipidemia (Kowluru and Chan, 2007) contributes to glial dysfunction and activation (gliosis) (Bringmann et al., 2006; Coorey et al., 2012), inflammation induced by resident glia (Müller cells), and death of the specific neuronal cell populations (retinal ganglion cells [RGCs]) (Ali et al., 2008), which intriguingly precede any observable clinical vascular irregularities or neuronal cell dysfunction in diabetes (Fletcher et al., 2007; Abcouwer and Gardner, 2014). However, although these studies highlight the premature changes that occur in the retina of diabetic patients, it is not clear whether glial cell abnormalities precede neuronal cell dysfunction or vice versa. Moreover, the pathophysiological events that bring about these changes remain ill defined, and currently no therapeutic strategies have been developed to counter them. Thus, it is important to understand these early changes in the neurovascular unit as they may be complementary to or even precede vascular abnormalities in diabetic patients.

The neurotrophin receptor p75 ($p75^{NTR}$), which is highly expressed in astrocytes and Müller cells in many models of neuronal damage, would be capable of mediating many of the pathological events described above. In retinopathies, such as glaucoma or optic nerve damage, $p75^{NTR}$ is upregulated and its ligand proNGF can promote production of inflammatory cytokines TNFα (Lebrun-Julien et al., 2009a; b, 2010; Bai et al., 2010a) and α2-macroglobulin (α_2M) from glial cells (Shi et al., 2008; Bai et al., 2011), which leads to RGC neurodegeneration. Moreover, $p75^{NTR}$ is known to contribute to cardiac vasculopathies (Siao et al., 2012), BRB breakdown, and fluid extravasation (Al-Gayyar et al., 2011; Mysona et al., 2013). These observations potentially place $p75^{NTR}$ at a crossroads of all pathological components of human DR: vascular defects, inflammation, and neurodegeneration. However, the mechanism by which $p75^{NTR}$ mediates these potentially sequential pathophysiological events during diabetes remains poorly understood.

Here, we use a streptozotocin (STZ)-induced mouse model of diabetes causing BRB breakdown with edema, inflammation, and RGC death; and an oxygen-induced retinopathy (OIR) mouse model to study pathological NV. We demonstrate a rapid and persistent increase of both proNGF and $p75^{NTR}$ at early stages of disease. The $p75^{NTR}$ increase occurs in Müller cell glia and in pericytes around the vasculature. $p75^{NTR}$ activity in Müller glia augments inflammatory cytokines TNFα and α_2M, which perform two paracrine functions. First, TNFα stimulates RGCs to secrete the vascular cue Semaphorin 3A, a soluble factor known to cause BRB breakdown and plasma extravasation (Cerani et al., 2013; Joyal et al., 2013). Second, TNFα and α_2M cooperate to promote RGC death in a proNGF and $p75^{NTR}$-dependent manner. Diabetes-induced BRB breakdown and edema, production of inflammatory cytokines, and RGC death are significantly diminished for prolonged periods upon acute administration of inhibitors of proNGF or $p75^{NTR}$; and both the vaso-obliteration (VO) and NV phases are significantly diminished in the mouse model of OIR. Thus, $p75^{NTR}$ and proNGF are key pathological mediators within the neuro-glia-vascular unit and may be potential therapeutic targets for various stages of DR pathology, including the DME, PDR, and neurodegenerative components; and offer an alternative to VEGF-based strategies to limit vascular abnormalities.

Materials and Methods

Animals. All experiments were conducted in accordance with Association for Research in Vision and Ophthalmology statement regarding use of animals in ophthalmic and vision research and were approved by all Institutional Animal Welfare Committees.

Female and male adult C57BL/6J (WT) mice were purchased from The Jackson Laboratory and coupled for litter production in the Animal Care facility at Maisonneuve-Rosemont Hospital Research Center (Montreal, Quebec, Canada). Adoptive CD-1 lactating females were purchased from Charles River Laboratories to tend to hyperoxia-exposed pups.

Induction of diabetes. Male 10-week-old mice (~24 g) received an intraperitoneal injection of STZ (60 mg/kg) (Sigma-Aldrich) dissolved in sodium citrate buffer (0.01 M, pH 4.5) on 5 consecutive days. After 1 and 6 weeks of injection with STZ, blood glucose was measured using a glucometer (Abbott Laboratory), and fasting blood glucose levels >17 mmol/L (300 mg/dl) (Mysona et al., 2013) were considered to be diabetic. Age-matched, nondiabetic C57BL/6 mice injected with sodium citrate buffer were used as controls. Fasting blood glucose levels were measured routinely. As example, a control group was 7.89 ± 0.69 mM, and the STZ group was 28.81 ± 4.204 mM ($p < 0.001$, $n = 12$).

OIR. Newborn mice pups were exposed for 5 d to 75% oxygen from postnatal day 7 (P7) to P12. VO and NV were assessed in hyperoxia-exposed mice pups at P12 and P17, respectively, as described previously (Smith et al., 1994; Stahl et al., 2010). Briefly, mice pups were fully anesthetized in 3% isoflurane in oxygen and killed using a guillotine. Eyes were enucleated and fixed in 4% PFA solution for 60 min at room temperature. Retinas were dissected and stained overnight at 4°C with fluorescein-labeled GSL 1, isolectin B4 (FL 1201, Vector Labs; 1:100). Lectin-stained retinas were whole-mounted onto Superfrost/Plus microscope slides (Fisher Scientific) with the photoreceptor side down and imbedded in Fluoro-gel (Electron Microscopy Sciences) and photomicrographed at 10× using a Zeiss AxioObserver.Z1. Images were photomerged into a single file using the MosiaX option in the AxioVision 4.6.5 software. Quantification of VO and NV was assessed using the SWIFT_NV methods as previously described (Stahl et al., 2009).

Optical coherence tomography (OCT) imaging. A noninvasive prototype spectrometer-based FD-OCT system was used to acquire the retinal images. FD-OCT is a noninvasive method that allows time-kinetic studies in the same animal, with axial resolution in tissue nominally better than 3 μm and repeatability of the measurements from B-scans better than 1 μm. Data acquisition was performed using custom software written in C^{2+} for rapid frame grabbing, processing, and display of 2D images (Li et al., 2011; Jian et al., 2013). B-scan images were segmented manually to quantify the thicknesses of the different retinal layers.

Mice were anesthetized using isoflurane/O_2 and placed on a platform, and the head was oriented to an angle at which the eye was properly aligned to the optical beam. The pupils were dilated with a topical solution (atropine sulfate 1%; Alcon). Refraction of light at the cornea was cancelled by placing over the eye a generic artificial tear gel. Alignment of the optical system to the mouse retina required a few minutes and was followed by rapid acquisition of data (~5 s/vol). During retinal scanning, three volumes were acquired in different sectors of the retina containing the ON head as landmark. After processing, three B-scans were randomly selected from each volume. The retinal thickness measurements were performed with MATLAB software (The MathWorks). In each B-scan, the thickness of the nerve fiber layer/ganglion cell layer (GCL)/inner plexiform layer (IPL), hereafter referred to as NGI (Saragovi et al., 1998; Bai et al., 2010a), was measured at three adjacent points. For each B-scan, the thickness of the inner nuclear layer (INL) and outer nuclear layer

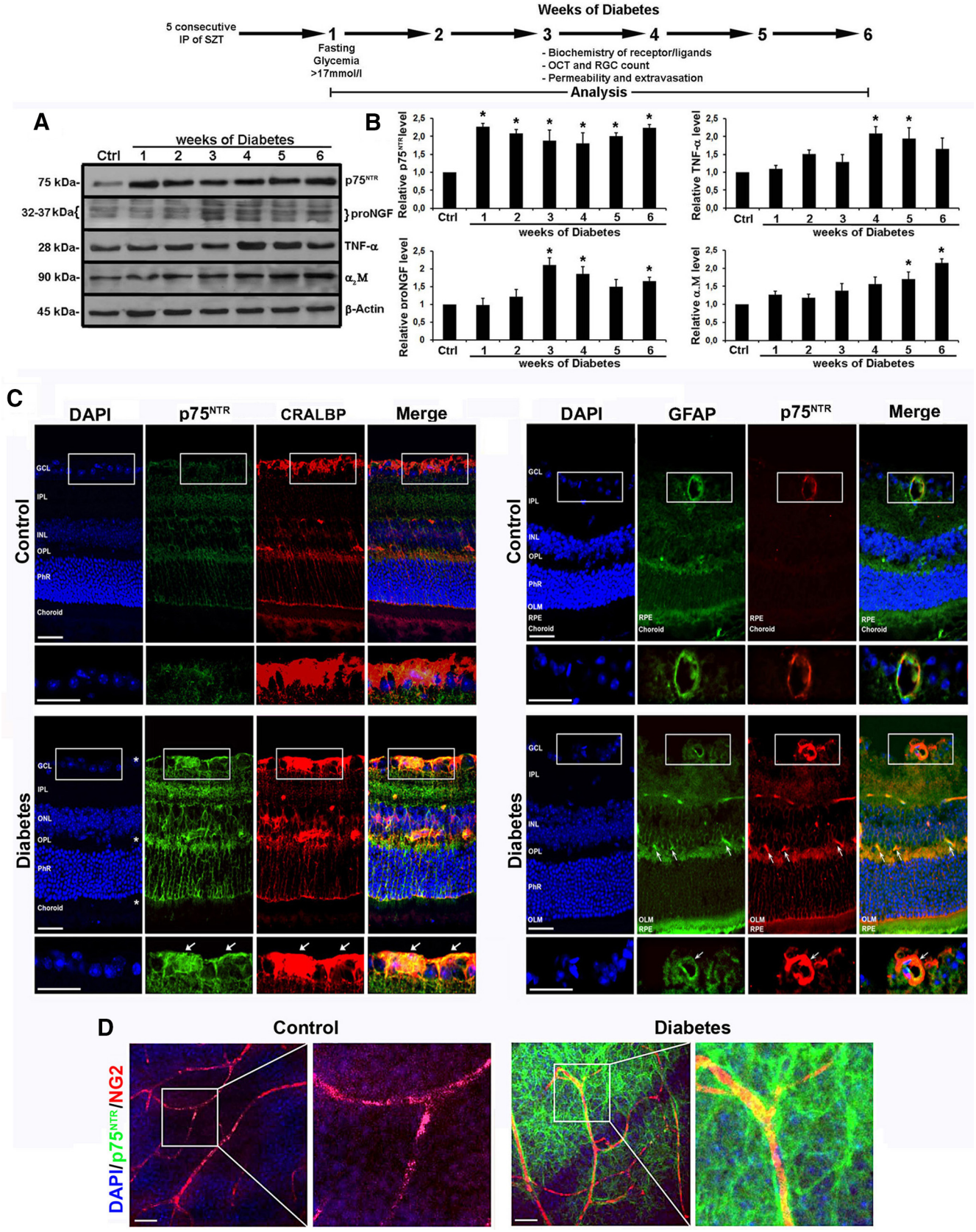

Figure 1. Expression and localization of p75 ^{NTR} and neurotoxic factors increase during the progression of DR. The experimental paradigm and the endpoints of the mouse DR model are shown. Drug treatments were injected intravitreally at week 2.5 of diabetes in this paradigm. ***A***, p75 ^{NTR}, proNGF, TNFα, and α_2M expression in whole mice retina analyzed by Western blot from 1– 6 weeks after induction of diabetes. There were increases of p75 ^{NTR} during week 1, of proNGF during week 3, of TNFα during week 4, and of α_2M during week 5. ***B***, Quantification. *$p < 0.05$, relative to control. $n = 3$ independent experiments, each with $n = 4$ mice/group. Statistical analysis was done by applying one-way ANOVA with significance established at $\alpha < 0.05$, followed by Bonferroni's correction for multiple comparisons. The 32–37 kDa bands of proNGF were quantified, and data are identical when the major band alone is quantified. ***C***, Confocal microscopy (*Figure legend continues.*)

(ONL), unaffected in the disease model, was also quantified as internal controls. Data are shown as average ± SEM thickness in micrometers (absolute values) in control versus diabetic-injected intravitreally once with either vehicle (PBS, 1% DMSO), THX-B, a pharmacological small-molecule antagonist of p75^{NTR} (Bai et al., 2010a; Mysona et al., 2013), or anti-proNGF NGF30 mAb (Saragovi et al., 1998; Bai et al., 2010a). THX-B is an antagonist of ligand-dependent and ligand-independent activity of p75^{NTR}, and a competitive blocker of proNGF binding to p75^{NTR}. The anti-proNGF mAb blocks proNGF binding to p75^{NTR}, as well as the binding of mature NGF to p75^{NTR}, but does not affect mature NGF binding or activity at TrkA.

Intravitreal injections. Mice were anesthetized in 3% isoflurane during intravitreal injections of clear solutions of THX-B p75^{NTR} antagonist, neutralizing anti-proNGF mAb, or vehicle. In the diabetes model, adult diabetic mice were injected at 2.5 weeks of diabetes. In the OIR model, mouse pups were injected at P7, P9, P12, or P14. All solutions were injected using a Hamilton syringe with 50 gauge glass capillary. The intraocular injections were in 2 μl volumes containing a total of 2 μg THX-B or 2 μg anti-proNGF NGF30 mAb as described for glaucoma (Shi et al., 2008; Bai et al., 2010a).

TUNEL assays and image analyses of flat-mounted retinas. The eyes were collected and retinas were dissected for flat-mounting and TUNEL staining; $n = 4$ mice per group. Control nondiabetic animals and diabetic animals were studied. One eye of each mouse was injected intravitreally once with either THX-B, or anti-proNGF mAb, or vehicle. Contralateral untreated eyes were used as control. Retinas were processed and stained with the DeathEnd Fluorometric TUNEL System as per the manufacturer's instructions (Promega). Briefly, whole retinas were dissected, fixed in 4% PFA overnight, and permealized with Proteinase K. Afterward, the samples were postfixed and the TdT reaction was carried on at 37°C in humidified chambers. TUNEL-labeled retinas were mounted with Vectashield-DAPI to counterstain nuclei. For each flat-mounted whole retina, three digital images per quadrant (superior, temporal, inferior, and nasal) were taken using confocal fluorescence microscopy at 20× magnification, for a total of 12 images per retina taken in a blinded fashion ($n = 4$ retinas per group). Images were taken at 0.5–0.7, 1.0–1.2, and 2.0–2.2 mm distances from the optic disc (areas 1, 2, and 3, respectively) and analyzed per area to account for known variations in RGC density in each area, as described previously (Bai et al., 2010a). Total TUNEL-positive cells and total nuclei of RGCs were counted in each picture. Each 20× magnification field exposes 0.2285 mm^2; and in each independent experiment, images spanning 10.97–21.93 mm^2 per group were analyzed.

RGC and fiber counts. The cornea, lens, and vitreous body were removed and the retina was dissected out for flat-mounting (Esquiva et al., 2013). After blocking (10% normal donkey serum in phosphate buffer plus 0.5% Triton X-100 for 1 h), the retinas were incubated for 72 h at 4°C with goat anti-Brn3a antibody (1:500; Santa Cruz Biotechnology) diluted in 0.1 M phosphate buffer containing 0.5% (v/v) Triton X-100 (Sigma) to detect the RGC population (García-Ayuso et al., 2010, 2015). After wash with phosphate buffer, the retinas were incubated overnight with the secondary antibody AlexaFluor-488 donkey anti-goat IgG (1:500; Invitrogen). Then, the retinas were washed and flat mounted in mounting medium (Citifluor) on glass slides with the GCL side up, and protected with a coverslip for optical microscopy. Using MetaMorph software (Leica MMAF 1.6) associated to a DMLA Microscope (Leica Microsystems) entire flat-mount retinas were photographed at 20× magnification. High-magnification pictures were taken using a laser-scanning confocal microscope (TCS SP2, Leica Microsystems). Brn3a-positive cells in the GCL were quantified at 0.5–0.7, 1.0–1.2, and 2.0–2.2 mm distances from the optic disc (areas 1, 2, and 3, respectively) using image-editing software (Photoshop 10.0; Adobe). Mean density (number of cells per mm^2) values were calculated for all the different areas. A total of 4 retinas per experimental group were analyzed.

FISH. The digoxigenin (DIG) RNA labeling kit (Roche) was used to generate the DIG-labeled probes. Efficient labeling was verified in agarose gels (1%). After enucleation, the eyes were immersed overnight in fixative at 4°C (4% PFA in PBS, pH 7.4), followed by cryoprotection in 30% sucrose overnight at 4°C. Eyes were embedded in OCT tissue TEK (VWR) and frozen with dry ice. Cryostat-cut sections (20 μm thick) were mounted onto gelatin-coated glass slides, refixed in 4% PFA, permeabilized with proteinase K, and acetylated. Hybridization was carried by incubating the slides with either 200 ng/ml of DIG-labeled TNFα or α_2M antisense RNAs probes overnight at 72°C in a hybridization oven (Robbins Scientific). As controls, hybridization with either 200 ng/ml of DIG-labeled TNFα or α_2M sense RNAs probes was performed on parallel slides using the same experimental conditions. Hybridization was followed by nonstringent and stringent washes, and incubation with anti-DIG-HRP (1:1000) overnight at 4°C. The amplification reaction was performed using the TMR-conjugated TSA kit (PerkinElmer) following manufacturer protocols. Finally, sections were washed and coverslipped using Vectashield mounting media with DAPI (Burlingame). The slides were analyzed by confocal microscopy.

Vascular permeability assay. Evans Blue permeation was analyzed by measuring albumin-Evans blue complex leakage from retinal vessels as previously described (Ma et al., 1996). Briefly, animals were injected intravenously with a solution of Evans blue (2% w/vdissolved in PBS). After 48 h, animals were killed, the whole eyes were enucleated, immediately embedded in OCT compound and cross sections were prepared. Microphotographs by immunofluorescence microscopy were obtained using identical exposure time, brightness, and contrast settings. For each experimental condition, at least 6 images were acquired from 3 sections cut from different areas of the retina ($n = 3$ retinas per group). The area of the Evans Blue permeation was measured using ImageJ software. For the *in situ* studies, an arbitrary rectangle was drawn that include all layer of the retina (GCL, IPL, INL, and ONL) to measure the Evans Blue staining using ImageJ. Data are shown as the average area (in pixels) ± SEM in control versus diabetic injected once with vehicle, anti-proNGF mAb, or small-molecule p75^{NTR} antagonist THX-B.

Immunohistochemistry. Whole eyes were enucleated from mice pups or adult and immediately fixed in 4% PFA at room temperature for 2 h. Eyes were saturated overnight at 4°C in a 30% sucrose solution before embedding in OCT compound (24608–930, TissueTek). Retinal cross sections of 10 μm were sectioned using a Cryostat (Leica). Sections were subsequently washed with PBS, permeabilized for 60 min at room temperature with 3% BSA, 0.2% Triton X-100, and 0.05% Tween20 in PBS, and stained with antibodies to mouse p75^{NTR} (1:1000; a kind gift from Dr. R. Rush) or rabbit p75^{NTR} (1:1000; a kind gift from Dr. P. Barker), rabbit glutamine synthetase (16802, Abcam; 1:200), mouse cellular retinaldehyde-binding protein (CRALBP, 15051, Abcam; 1:1000), rabbit GFAP (AB5804, Millipore, 1:1000), rat anti-proNGF/NGF mAb NGF30 (1:2000) (Saragovi et al., 1998; Bai et al., 2010a) prepared in house, rabbit TNFα (AB2148P, Millipore, 1:1000), rabbit α_2M (1:1000, Santa Cruz Biotechnology) or mouse βIII-tubulin (T8578, Sigma-Aldrich; 1:1000). Fluoresceinated secondary antibodies (goat anti-mouse IgG AlexaFluor-488, -594, and/or -647 and goat anti-rabbit IgG AlexaFluor-488, -594, and/or -647; Invitrogen) were used for localization studies according to manufacturers' recommendations. Images were obtained using an IX81 confocal microscope (Olympus) equipped with Fluoview 3.1 software (Olympus). As controls during immunostaining, adjacent sections were processed equally but without primary or with irrelevant primary, followed by the proper secondary. In all cases, background levels are undetectable.

Western blot. Eyes were enucleated and retinas immediately dissected and placed into protein lysis buffer and briefly homogenized. Samples (combined retinal lysate from two different animals) were centrifuged and 30 μg resolved on an SDS-PAGE gel (8%–12%) and electro-blotted

←

(*Figure legend continued.*) images show induction and distribution of p75^{NTR} in mice retina after 6 weeks of diabetes compared with age-matched control animals. p75^{NTR} (red) was preferentially expressed in Müller cells (green, white arrows in insets pointing at the end-feet of Müller cells), as revealed by coexpression with CRALBP, and around the vessels where p75^{NTR} (red, white arrows in insets pointing at the vessels in the outer plexiform layer) was coexpressed with GFAP, a specific marker of active Müller and astrocyte cells (green). Nuclei are counterstained with DAPI. White rectangles represent magnified areas (40×) shown in the insets. Scale bar, 30 μm. PhR, Photoreceptor layer; OLM, outer limiting membrane; RPE, retinal pigment epithelium. ***D***, Flat-mounted retinas from the same animals show partial colocalization of p75^{NTR} (green) with NG2 (red) pericyte marker around vessels. Scale bar, 100 μm.

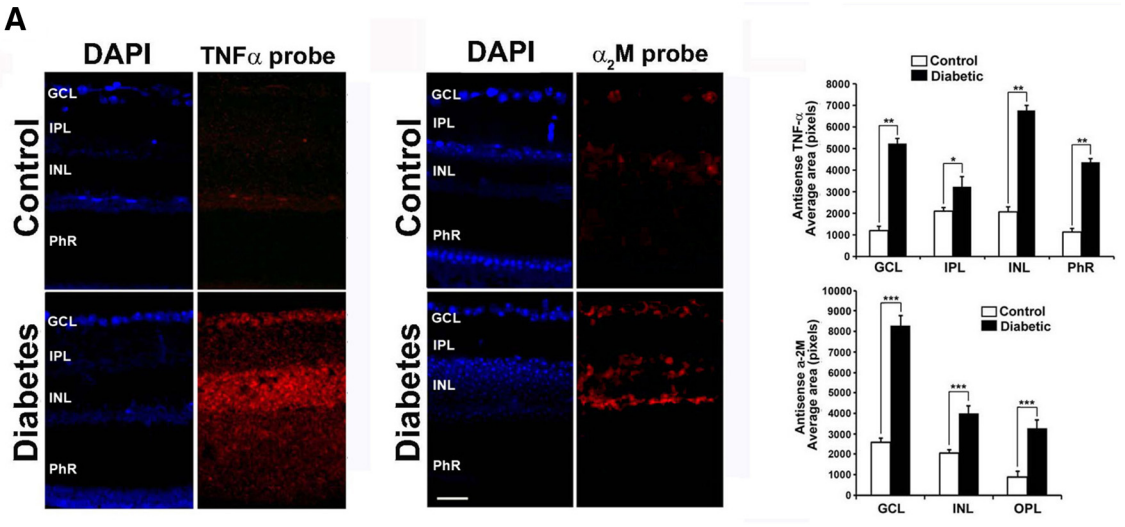
A
DAPI
TNFα probe
DAPI
α2M probe
Control
Diabetes
GCL
IPL
INL
PhR
Control
Diabetic
Antisense TNF-α Average area (pixels)
Antisense α2M Average area (pixels)
GCL
IPL
INL
PhR
OPL

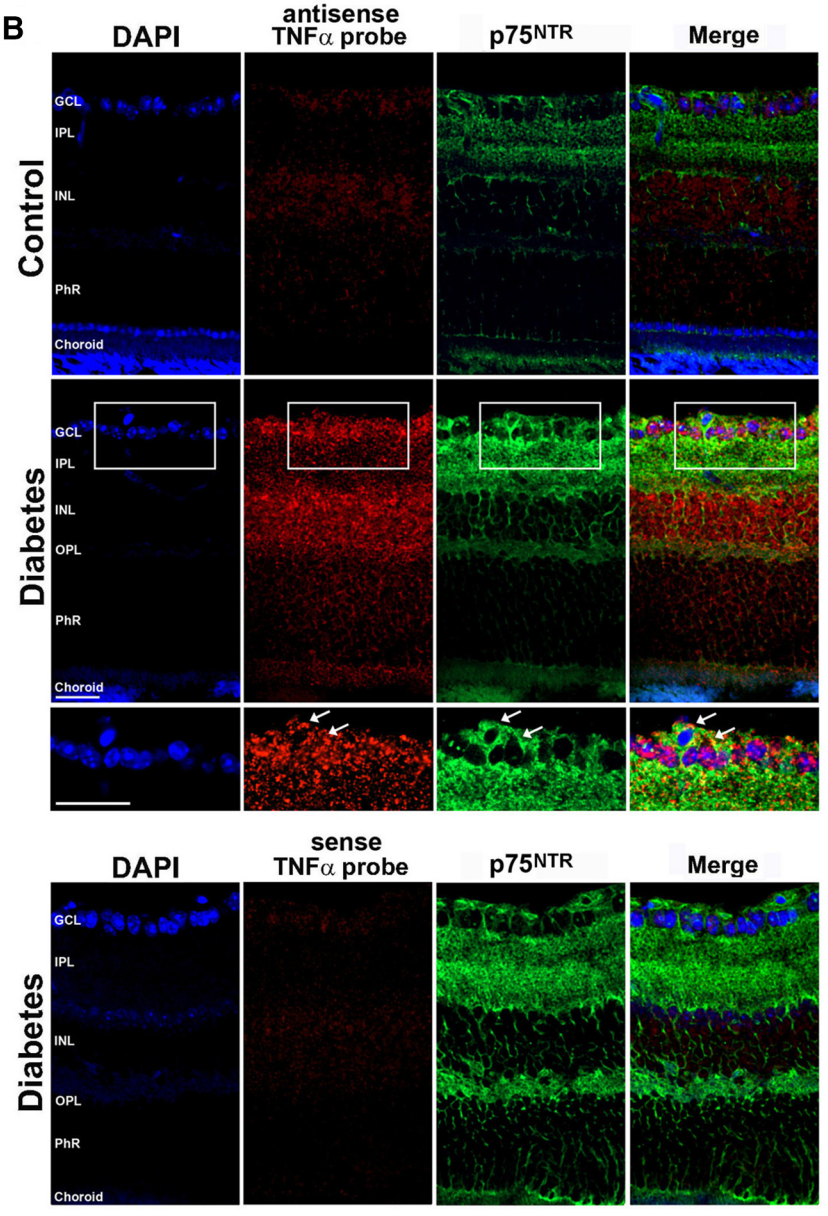
B
DAPI
antisense TNFα probe
p75NTR
Merge
Control
Diabetes
GCL
IPL
INL
OPL
PhR
Choroid
sense TNFα probe

onto either PVDF or nitrocellulose membranes (Bio-Rad). Membranes were washed, blocked for 60 min in 5% milk in TBS-Tween, and incubated overnight at 4°C with mouse antibody to β-actin (sc-47778, Santa Cruz Biotechnology; 1:1000), rabbit antibody to $p75^{NTR}$ (1:1000; a kind gift from Dr. P. Barker), rabbit TNFα (AB2148P, Millipore, 1:2000), rabbit α_2M (Santa Cruz Biotechnology; 1:2000), and rat proNGF/NGF (1:200). After washing, membranes were incubated with 1:5000 HRP-conjugated anti-mouse or 1:2000 HRP anti-goat or -rabbit secondary antibodies (Millipore) for 2 h at room temperature. Membranes were imaged with LAS-3000 imager (FujiFilm), and bands were assessed using densitometry plugins in Multi Gauge 4.0 software (FujiFilm). The size of bands reported are M_r calculated using standard markers.

Cell culture. Rat brain microvascular endothelial cells (RBMVECs) were obtained from Cederlane Laboratories and used between passages 2–7. rMC-1 cells were cultured in low glucose DMEM (Invitrogen) supplemented with 10% FBS and 1% penicillin/streptomycin at 37°C and 5% CO_2, whereas RBMVECs were cultured as described by manufacturer's instructions. Cells were starved 4 h before treatment with 0.1, 1.0, or 10.0 ng/ml of recombinant proNGF (CYT-426, ProSpec). Neutralizing antibody to proNGF was used at 1 μg/ml, whereas THX-B was used at 4 μg/ml. Proteins were extracted using protein lysis buffer and lysates processed for Western blot analysis. Total RNA was isolated using TriZol (Invitrogen) and analyzed via RT-PCR and qPCR analysis.

Reverse-transcription PCR and quantitative real-time PCR. Cell culture and retinas samples were processed using TriZol (Invitrogen) as described by the manufacturer's instructions. Subsequently, genomic DNA was removed using DNase I (Invitrogen) as described by the manufacturer's instructions. Total RNA (1 μg) was reverse-transcribed into cDNA using iScript RT Supermix (Bio-Rad) following the indications of the manufacturer. cDNA was analyzed by quantitative real-time PCR on the ABI 7500 Real-Time PCR system (Applied Biosystems) and using iQ SYBR Green Supermix (Bio-Rad) with primers targeting Semaphorin 3A, TNFα, and β-actin (designed using primer3 [NCBI]). The primers were used to generate specific fragments: rat TNFα forward, 5′ CTAT GTGCTCCTCACCCACA 3′, reverse 5′ TGGAAG ACTCCTCCCAGG TA 3′; mouse TNFα forward, 5′ GAGTCCCAGGTCTACTTT 3′, reverse 5′ CAGGTCACTGTCCCAGCATCT 3′; and mouse Semaphorin 3A forward, 5′ GGGACTTCG CTATCTTCAGAAC 3′, reverse, 5′ GGCGT-GCTTTTAGGAATGTTG 3′. All primers were used at 100 nM. The reaction was performed in triplicate with an Mx3000P QPCR System (Stratagene). Amplification reaction data were analyzed using the complementary Mx3000P analysis software. Target gene expression was normalized to the average expression of the housekeeping gene GAPDH forward 5′ CACCACCTTGATGTCATC-3′, reverse 5′AGCCCAGAAC ATCCCTG3′. Quantitative analysis of gene expression was assessed using the ΔΔCT quantification.

Preparation of rMC-1 conditioned media (CM). rMC-1 were seeded (10^6 cells) and starved 4 h before treatment with 1.0 ng/ml of recombinant proNGF (CYT-426, ProSpec). Supernatants were collected 24 h later, cleared by centrifugation, filtered through 0.22 μm filters (Millipore), and distributed for cell survival assays (see below).

Cell survival assay. Approximately 10^4 RBMVEC cells/well were seeded in 24 well plates and starved 4 h before exposure to rMC-1 CM. Neutralizing antibody to proNGF was used at 1 μg/ml, whereas THX-B was used at 4 μg/ml. After 24 h, 50 μl of a 5 μg/ml solution of thiazolyl blue tetrazolium bromide (M2128; Sigma) was added to each well and cells incubated for 2–3 h. Subsequently, the supernatant was aspirated and cells were lysed and resuspended in acidified isopropanol and shaken for 5 min. Duplicate absorbance readings were taken at 565 nm using Infinite M1000 Pro plate reader (TECAN).

Statistical analysis. Results are presented as mean ± SEM for all studies. One-way or two-way ANOVA with significance $\alpha = 0.05$ or higher were used for processing data. Bonferroni *post hoc* analysis was used for calculating significance between groups. Two-tailed Student's *t* tests were used to test for significance between two means.

Results

Upregulated retinal $p75^{NTR}$ and proNGF in a mouse model of Type 1 diabetes is followed by induction of proinflammatory cytokines

To study the effects of $p75^{NTR}$ and its ligand proNGF in DR, we determined their expression pattern in a STZ mouse model of Type 1 diabetes mellitus. Time-kinetic studies were performed by quantitative Western blots on retinas collected from diabetic animals between weeks 1–6 following diabetes onset. At week 1 of diabetes, retina $p75^{NTR}$ protein levels rose ~2-fold compared with control retinas ($p < 0.05$, $n = 4$). Retina proNGF protein expression increased ~2-fold at week 3 of diabetes compared with control retinas ($p < 0.05$, $n = 4$). Significantly higher retinal levels of $p75^{NTR}$ and proNGF persisted for at least 6 weeks of diabetes compared to control retinas (Fig. 1*A*, quantified in Figure 1*B*).

In some retinal neurodegenerative diseases, such as optic nerve axotomy or glaucoma, proNGF-mediated toxicity affects non–$p75^{NTR}$-expressing cells, suggesting a non–cell-autologous process. Indeed, in human and rodent disease, $p75^{NTR}$ and proNGF upregulate two proteins α_2M (Bai et al., 2010a, b, 2011) and TNFα (Lebrun-Julien et al., 2009a, 2010; Bai et al., 2010a, b, 2011) secreted from Müller glia, which contribute to neurodegeneration (Bai et al., 2011; Barcelona and Saragovi, 2015).

Hence, we studied these proteins as a putative mechanism that can perturb glial function, induce neuronal apoptosis, and cause vascular perturbations in the STZ model of diabetes. In diabetic retinas, α_2M protein levels increased ~1.5-fold at week 5 compared with controls (α_2M, 1.641 ± 0.149; $p < 0.05$, $n = 4$) and TNFα protein levels surged ~2-fold increase at week 4 compared with controls (TNFα, 2.12 ± 0.193; $p < 0.05$, $n = 4$) (Fig. 1*A*, quantified in Figure 1*B*). Essentially, sequential upregulation of $p75^{NTR}$ and proNGF is associated time-dependently with an increase in TNFα and α_2M that can be proinflammatory and neurotoxic.

Retinal $p75^{NTR}$ is upregulated in activated Müller cells, astrocytes, and vascular pericytes in a mouse model of Type 1 diabetes

Immunohistochemical studies in retinal sections demonstrated increased expression of $p75^{NTR}$ in Müller cells identified by CRALBP; and in the periphery of vessels, the nerve fiber and GCLs, and Müller cell end-feet and astrocytes labeled with GFAP (Fig. 1*C*). $p75^{NTR}$ levels were significantly elevated in diabetic retinas compared with control animals, which corroborates the Western blot analysis. The elevated $p75^{NTR}$ label in the periphery of vessels of diabetic retinas seen in cross sections was studied in whole flat-mounted retinas. The elevated $p75^{NTR}$ label corresponds to vascular pericytes also labeled with the NG2 marker (Fig. 1*D*). In these whole flat-mounted retinas, the $p75^{NTR}$ label (green) that appears beneath the pericytes corresponds to Müller cell fibers and astrocytes. Similar data were obtained using other pericyte markers (PDGF-receptor; data not shown).

←

Figure 2. The expression of the cytotoxic molecules TNFα and α2M is increased in Müller cells during DR. ***A***, FISH shows induction and distribution of DIG-labeled TNFα or α_2M antisense RNAs probes (red) in mice retina after 6 weeks of diabetes compared with age-matched control animals. Nuclei are counterstained with DAPI. Scale bar, 30 μm. Histograms represent the quantification of the expression of TNFα and α_2M mRNAs in the GCL, IPL, INL, outer plexiform layer (OPL), and photoreceptor layer (PhR). Statistical analysis was done by applying one-way ANOVA with significance at $\alpha < 0.05$. *$p < 0.05$, relative to control. **$p < 0.01$, relative to control. ***$p < 0.001$ relative to control. $n = 3$ independent experiments, each with $n = 4$ mice/group. ***B***, FISH followed by immunofluorescence showing colocalization of TNFα mRNAs (red) with $p75^{NTR}$ protein (green) in the end-feet of Müller cells (white arrow, insets) and in the IPL. Scale bar, 30 μm. White rectangles represent higher-magnification images (40×) represented in the insets. Sense TNFα mRNA hybridization was used on diabetic retina samples as a negative control.

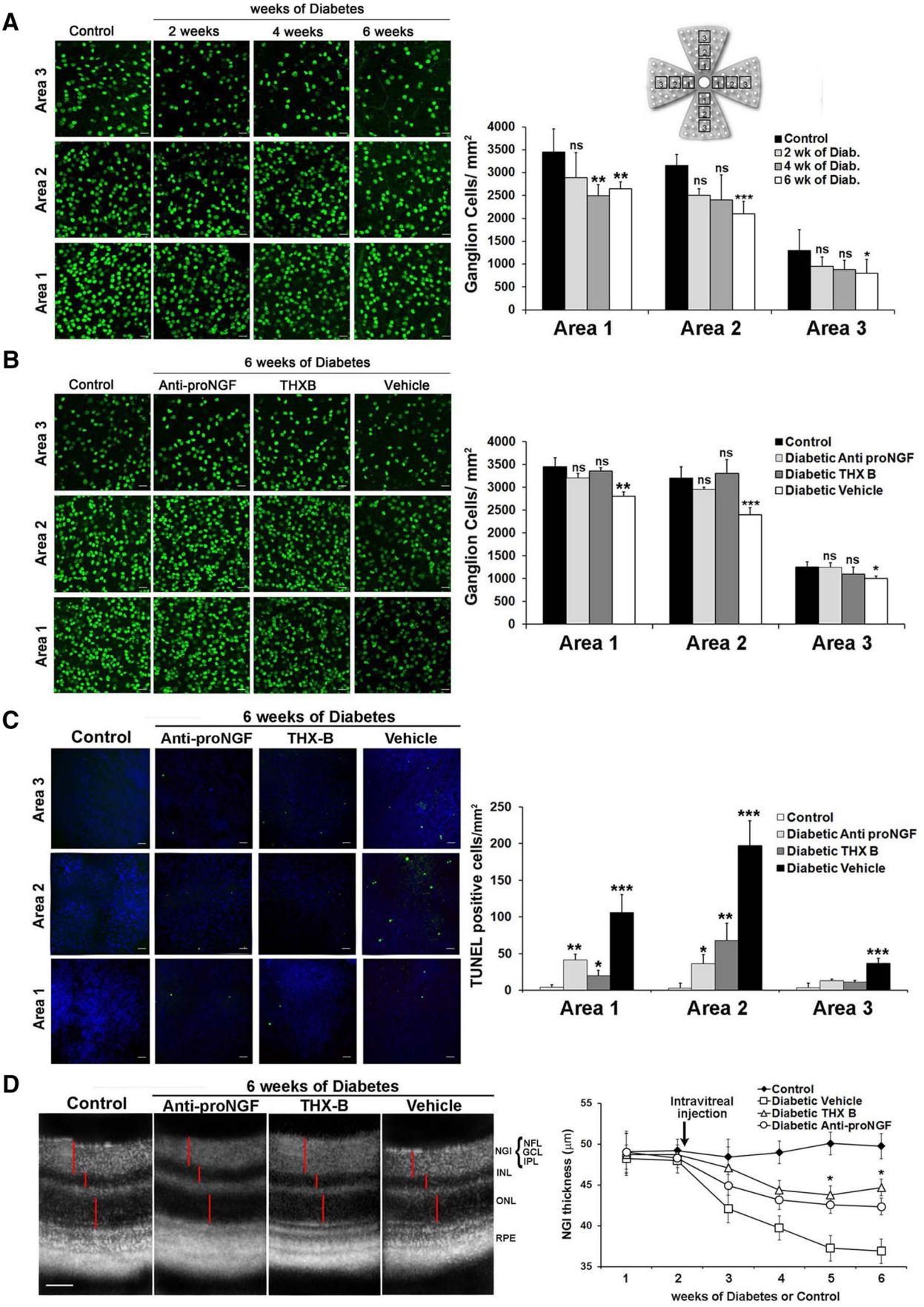

Figure 3. Pharmacological inhibition of p75 ^{NTR} or proNGF preserves retinal structures where RGCs are located and inhibits RGC death in DR. ***A***, Representative images of Brn3-labeled RGCs from 3 different retinal areas at concentric distances from the optic nerve: 0.5– 0.7 mm (area 1), 1.0 –1.2 mm (area 2), and 2.0 –2.2 mm (area 3). RGCs were quantified in (*Figure legend continues.*)

α_2M and TNFα mRNA in diabetes is upregulated primarily in Müller glial cells

Because α_2M and TNFα are soluble factors, to determine their cellular expression patterns, we performed *in situ* mRNA hybridization on retinal sections of mice 6 weeks after STZ. Our results demonstrate significant increases in TNFα mRNA in the RGC layer ($p < 0.01$), IPL ($p < 0.05$), INL ($p < 0.01$), and photoreceptor layer ($p < 0.01$) compared with control retinas (Fig. 2*A*). Interestingly, most of the diabetes-induced upregulation of TNFα mRNA was seen in the RGC layer and INL, the main retinal layers affected in DR. Furthermore, there was an increase in α_2M mRNA in the RGC layer and INL. Upregulation of α_2M mRNA was also detected in the boundary between the INL and photoreceptor layers, likely associated with cells of the retinal vasculature in that location (Fig. 2*A*). Graphs show significant changes quantified for TNFα and α2M mRNAs in each retinal layer.

Some of the TNFα mRNA signal in the RGC layer colocalizes with p75^{NTR} protein in what are likely Müller cell end-feet. Control hybridization with TNFα sense mRNA probes showed undetectable levels, confirming the specificity of the technique (Fig. 2*B*). Similar controls were obtained using α_2M sense probes (data not shown).

Together, these data suggest that, in diabetic retinas, p75^{NTR}, expressed mainly on Müller glia and astrocytes, contribute to the production of α_2M and TNFα, which can be proinflammatory and. neurotoxic and may contribute to the pathogenesis of diabetes through a paracrine mechanism.

Pharmacological inhibition of p75^{NTR} or proNGF in diabetes reduces RGC death and preserves retinal structures

Next, we evaluated whether elevated expression of p75^{NTR} in Müller glia, astrocytes, and pericytes impact neurodegeneration associated with DR progression. To do this, we quantified RGC-specific Brn3 staining, TUNEL staining, and OCT measurements of retinal structure in diabetic retinas with or without therapeutic treatment with a p75^{NTR} small-molecule antagonist (THX-B) or an anti-proNGF blocking mAb (Fig. 3) previously described as having potent p75^{NTR} inhibitory properties (Bai et al., 2010a). Analyses and quantification were done at specified distances from the optic disc (areas 1, 2, and 3, respectively) to account for normal thinning of RGC density toward the periphery. After 6 weeks of diabetes, there was an ~15%-25% reduction in Brn3$^+$ RGCs in flat-mounted whole retinas, compared with control naive retinas (area 1: 3450 ± 413 vs 2787 ± 219 cells/mm^2, $p < 0.05$; area 2: 3215 ± 284 vs 2095 ± 250 cells/mm^2, $p < 0.01$) (Fig. 3*A*).

To test whether RGC loss in diabetic retinas is p75^{NTR}- or proNGF-dependent, animals were injected THX-B or anti-proNGF mAb into the vitreous 2.5 weeks following onset diabetes (contralateral eyes were injected with vehicle control). Treatment with anti-proNGF mAb or THX-B preserved the Brn3$^+$ RGCs counted at week 6 of diabetes (area 1: 3202 ± 123 and 3350 ± 98 cells/mm^2, respectively, vs 2786 ± 279 cells/mm^2 vehicle-treated contralateral eyes, $p < 0.05$; area 2: 2944 ± 129 and 3310 ± 378 cells/mm^2, respectively, vs 2416 ± 194 cells/mm^2 vehicle-treated contralateral eyes, $p < 0.001$ and $p < 0.05$, respectively) (Fig. 3*B*).

To consolidate these results, we performed TUNEL staining on retinal flat mounts obtained from 6 week diabetic mice that had been injected 2.5 weeks following onset diabetes with THX-B, proNGF mAb, or vehicle. TUNEL-positive staining was significantly diminished in eyes receiving intravitreal injections of THX-B or anti-proNGF mAb compared with vehicle-treated contralateral eyes (Fig. 3*C*; $p < 0.05$). The analyses of flat-mounted retinas quantify the RGC layer containing RGC nuclei, displaced amacrine cells, and astrocytes. Because astrocytes do not die in this disease model, the TUNEL$^+$ cells can only be RGC neurons or displaced amacrine cells.

These data indicate that the reduced numbers of Brn3$^+$ RGCs in diabetic retinas occurs in a p75^{NTR}-dependent manner, an outcome prevented by inhibition of p75^{NTR} activity using THX-B or anti-proNGF mAb. Moreover, the fact that p75^{NTR} is not expressed in RGCs suggest a non–cell-autonomous mechanism.

Further RGC layer quantification was performed by OCT, a noninvasive method for measuring structural changes *in vivo*, and which correlates with RGC numbers during neurodegeneration (Sarunic et al., 2010). OCT was performed longitudinally in animals from 1 to 6 weeks following onset of diabetes, measuring RGC cell bodies and fibers in the nerve fiber layer, the GCL, and the IPL termed NGI (Fig. 3*D*). In diabetic eyes, the NGI thickness decreased progressively and was significantly lower after 5 weeks of diabetes compared with age-matched nondiabetic eyes (37.85 ± 1.3 μm vs 50.45 ± 0.9 μm; $p < 0.05$).

Treatment of diabetic eyes with anti-proNGF mAb or THX-B protected against NGI thinning (42.51 ± 1.7 μm and 43.75 ± 1.1 μm, respectively, $p < 0.05$ vs vehicle-treated contralateral diabetic eyes). Structural preservation of NGI by anti-proNGF mAb or THX-B were still significant after 6 weeks of diabetes (42.42 ± 0.9 μm and 44.67 ± 1.9 μm, respectively; vs vehicle-treated contralateral diabetic eyes 37.11 ± 1.5 μm, $p < 0.05$) (Fig. 3*D*).

As internal controls, we quantified retinal layers that do not change in diabetes (INL, containing the Müller and bipolar cell bodies) as well as the cone and rods of photoreceptors that make up the ONL. Combined, these data indicate that, in the retinas of diabetic mice, ligand-dependent p75^{NTR} activity promotes effectors that contribute to RGC death, with resulting retinal structural changes specifically in the NGI. Given the significant and selective loss of the nerve fiber layer thickness, which comprises RGC axons and fibers, most of the TUNEL$^+$ cells must be RGCs.

In sum, a single injection of an antagonist of p75^{NTR} or proNGF, at week 2.5 of diabetes and with concurrent pathology, prevents structural degeneration and RGC apoptosis for prolonged periods lasting to at least week 6 of continuing diabetes.

←

(*Figure legend continued.*) flat-mounted retinas at 2, 4, and 6 weeks after induction of diabetes. Scale bar, 20 μm. *$p < 0.05$ versus control naive mice. **$p < 0.01$ versus control naive mice. ***$p < 0.001$ versus control naive mice. ***B***, Representative images of Brn3-labeled RGCs in flat-mounted retinas in 6 week diabetic mice ± treatment at week 2.5 of diabetes with anti-proNGF mAb, or THX-B, or vehicle, compared with age-matched naive control animals. Scale bar, 20 μm. Anti-proNGF mAb or THX-B treatment prevents loss of RGCs in all areas: area 1, **$p < 0.01$ (repeated-measures ANOVA); area 2, ***$p < 0.001$ (repeated-measures ANOVA); area 3, *$p < 0.05$ (repeated-measures ANOVA). ***C***, Representative pictures of TUNEL$^+$ cells in 6 week diabetic mice ± treatment at week 2.5 of diabetes with anti-proNGF mAb, or THX-B, or vehicle, compared with age-matched naive control animals. Anti-proNGF mAb or THX-B was significantly protective in all three areas. ***$p < 0.001$ (repeated-measures ANOVA). ***D***, Representative sections of B-scan OCT images in 6 week diabetic mice ± treatment at week 2.5 of diabetes with anti-proNGF mAb, or THX-B, or vehicle, compared with age-matched naive control animals. Histogram represents time-dependent changes in the thickness of the NGI layer ± SD ($n = 3$ eyes). Note the progressive loss of NGI thickness in the vehicle-treated diabetic vehicle retina. The NGI layers are where the RGCs bodies and RGC fibers are located, whereas the structure of the other layers (INL and ONL) do not change (see vertical red bars). Anti-proNGF mAb or THX-B treatment significantly protected the NGI layer structure at weeks 5 and 6. *$p < 0.05$ (two-way ANOVA with significance established at $\alpha < 0.05$, followed by Bonferroni's correction for multiple comparisons). ns, Not significant.

p75^{NTR}-proNGF signaling axis in diabetes augments TNFα and α_2M neurotoxin release, which contribute to RGC loss

To elucidate the mechanism by which p75^{NTR}-proNGF signaling mediates neuronal apoptosis, we studied levels of TNFα and α_2M. The levels of TNFα mRNA were quantified by qPCR at 6 weeks of diabetes versus control. TNFα mRNA levels increased ~2-fold in diabetic mice (2.24 ± 0.221; $p < 0.001$ $n = 3$ mice per group). In diabetic eyes treated with anti-proNGF mAb or THX-B, however, TNFα mRNA levels were significantly lower compared with vehicle-treated contralateral diabetic eyes (1.21 ± 0.145, $p < 0.01$, or 1.59 ± 0.421, $p < 0.01$, respectively, $p < 0.01$, $n = 3$ mice per group; Fig. 4*A*). Indeed, in diabetic eyes treated with anti-proNGF mAb or THX-B, TNFα mRNA levels were not statistically different from normal naive control retinas.

Given that TNFα mRNA is expressed in Müller glia (Fig. 2), we studied proNGF/p75^{NTR} regulation of TNFα in the rat Müller cell line rMC-1 that express p75^{NTR} (Barcelona and Saragovi, 2015), by qPCR. Treatment of rMC-1 cells for 24 h with recombinant proNGF caused increases in TNFα mRNA, in a dose-dependent manner (Fig. 4*B*). This effect was abrogated with cotreatment with either THX-B or anti-proNGF mAb (Fig. 4*C*; $p < 0.001$ and $p < 0.01$, respectively). Control treatments with THX-B alone or anti-proNGF mAb alone did not affect baseline TNFα expression.

The TNFα mRNA increase caused by proNGF is consistent with reported TNFα protein increase caused by proNGF in the rMC-1 cell line (Barcelona and Saragovi, 2015). Moreover, it is reported that proNGF and α_2M synergize to stimulate production of TNFα protein in the rMC-1 cell line (Barcelona and Saragovi, 2015).Hence, we quantified TNFα and α_2M protein in normal and diabetic retinas. TNFα and α_2M protein levels were significantly increased in retinas of 6 week diabetic mice compared with naive control mice (Fig. 4*D*). The increase in diabetic animals was significantly reduced by treatment with anti-proNGF mAb or THX-B compared with vehicle-treated contralateral diabetic eyes ($n = 3$ mice per group). However, it is noteworthy that, following treatment with anti-proNGF mAb or THX-B, the p75^{NTR} expression remained elevated, whereas treatment with anti-proNGF mAb reduced the levels of proNGF (Fig. 4*D*).

Immunohistochemical analysis of retinal sections from animals treated with anti-proNGF mAb or THX-B demonstrated attenuation in TNFα protein accumulated in and around the end-feet of CRALBP-positive Müller cells and in the RGC layer (Fig. 4*E*). Reduction of α_2M immunostaining was also observed in the proximity of vessels in all layers (Fig. 4*F*). These results indicate that pharmacological inhibition of p75^{NTR} or its proNGF agonist attenuates retinal proinflammatory cytokines secreted by Müller glia and other cells, which has the positive effect of ameliorating neurodegeneration in diabetic mice.

Inhibition of p75^{NTR} or proNGF efficiently reduces pathological vascular permeability in diabetic mice by affecting Sema3A production in neighboring RGCs

Knowing that increased p75^{NTR} activity promotes glial activation and production of inflammatory cytokines (Fig. 4) and RGC death (Fig. 3), we next explored how these events might impact BRB breakdown and edema, an important pathophysiological phenomenon of diabetic pathology.

Semaphorin3A (Sema3A) has been previously shown to induce BRB breakdown in diabetic mice (Cerani et al., 2013), and its expression is increased in RGCs by proinflammatory cytokines (Joyal et al., 2013). To test whether TNFα triggers Sema3A, we treated the RGC5 neuronal cell line with recombinant TNFα, which significantly augmented Sema3A mRNA ~2-fold after 4 h ($p < 0.001$) (Fig. 5*A*).

At 8 weeks of diabetes, there is a significant ~4-fold increase in Sema3A mRNA ($p < 0.001$ compared with naive control retinas). This Sema3A mRNA is presumably promoted by increased TNFα levels in diabetes. Because increased TNFα levels in diabetes are promoted by p75^{NTR} activity, we tested whether treatment with anti-proNGF mAb or THX-B, injected intravitreally at week 2.5 of diabetes, affected Sema3A mRNA levels. Treatment caused a partial but significant reduction in Sema3A mRNA compared with vehicle-treated contralateral diabetic eyes ($p < 0.01$, $n = 3$) (Fig. 5*B*); from ~4-fold to ~2.5-fold. However, Sema3A levels are not normalized and remain significantly higher than in normal naive control retinas.

Lower Sema3A production during diabetes leads to diminished BRB breakdown and reduced Evans blue vascular leakage at 8 weeks of diabetes. Intravitreal injections of anti-proNGF mAb or THX-B, at week 2.5 of diabetes, caused 85% and 65% decrease in vascular leakage, respectively ($p < 0.001$ compared with vehicle-treated contralateral diabetic eyes, $n = 3$ independent experiments with a total of 12 mice) (Fig. 5*C*). It should be noted that extravasation of fluid from the vasculature contains high levels of α_2M, which is present in serum at a concentration of 2–4 mg/ml (Barcelona and Saragovi, 2015). Importantly, reducing extravasation also helps to prevent α_2M (and perhaps other factors) from reaching the retinal stroma after BRB breakdown.

In sum, proNGF and p75^{NTR}-dependent Müller cell glia local production of TNFα and α_2M stimulates Sema3A production by RGCs, leading to BRB breakdown and edema, with further accumulation of serum components, such as α_2M, which potentiate inflammation and cause RGC death. All these events can be ameliorated using antagonists of proNGF or p75^{NTR}.

Pharmacological inhibition of p75^{NTR} diminishes oxygen-induced VO and inhibits microvascular endothelial cell death

VO and NV take place in human diabetes; however, the phase of pathological NV does not occur in the mouse STZ model. Hence, we used the well-established mouse model of OIR to elucidate the role of p75^{NTR}-proNGF signaling axis during the VO and NV phases of disease. Mouse pups were exposed to 75% oxygen for 5 d (from P7 to P12), and retinal levels of p75^{NTR}, NGF, and proNGF protein were quantified by Western blot. During the VO phase, proNGF was significantly increased ($p < 0.001$) and mature NGF was significantly decreased ($p < 0.001$) (Fig. 6*A*). In contrast, there was no change in p75^{NTR} expression (Fig. 6*A*), which may be attributed to already elevated baseline levels of p75^{NTR} normally required for retinal pruning and development during the first 14 d of postnatal life (Frade et al., 1999).

Next, to determine whether p75^{NTR} activity was relevant in VO, mice were injected intravitreally with THX-B at P7 OIR (because VO occurs within the first 48 h). THX-B-treated pups displayed significantly less VO ($p < 0.01$) compared with vehicle-injected OIR pups at P12 OIR (Fig. 6*B*). These results are consistent with our data on diabetic animals treated with THX-B or anti-proNGF mAb, which also showed reduced vascular pathology, decreased levels of TNFα and Sema3A, reduced RGC death and structural changes in the NGI layer, and reduced BRB breakdown.

We next set out to determine whether p75^{NTR}-dependent VO in OIR is mediated by TNFα and whether protection of VO by THX-B occurs via inhibition of TNFα and/or Sema3A.

Quantitative PCR at P9 showed significantly reduced production of both retinal TNFα mRNA ($p < 0.001$) and Sema3A

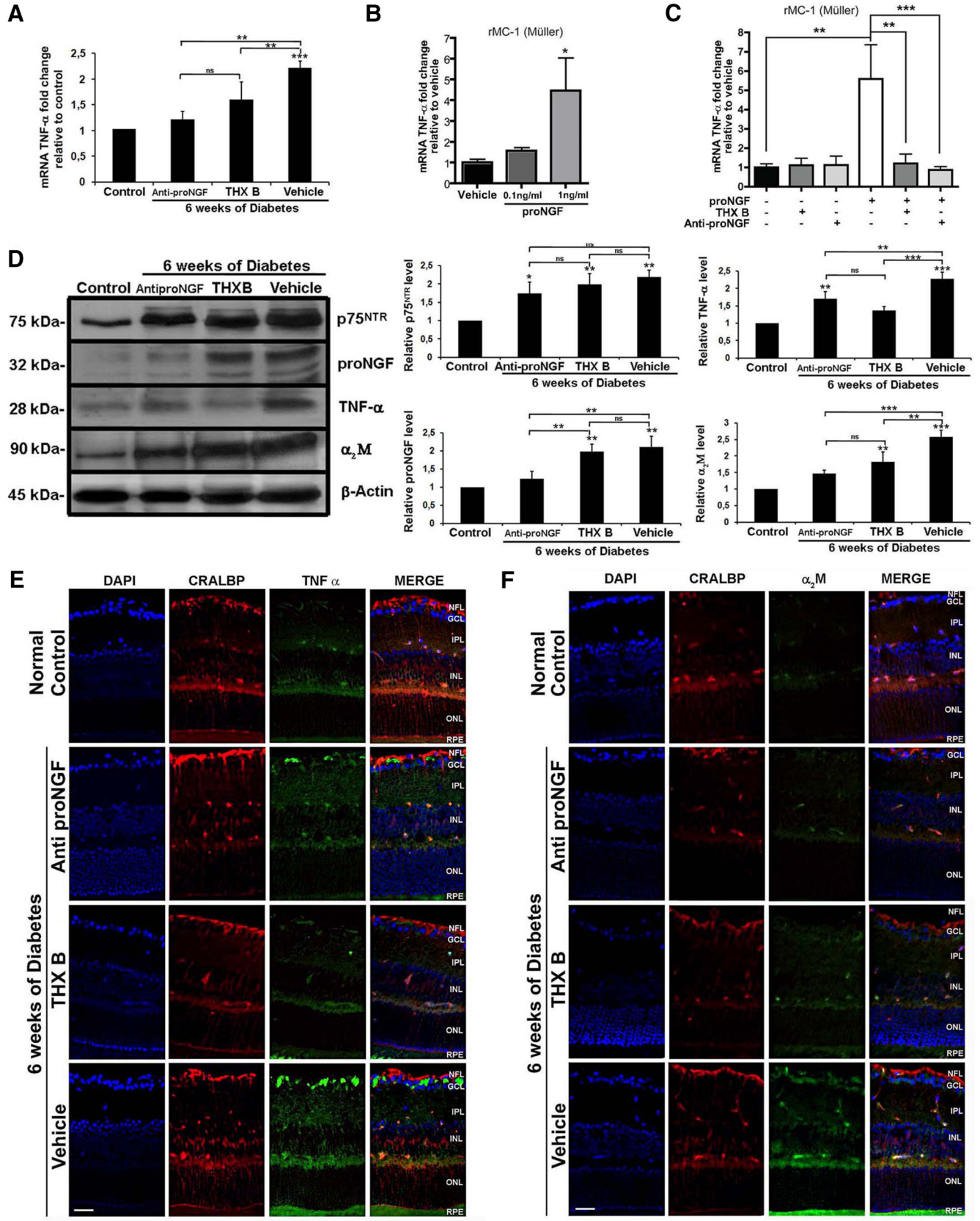

Figure 4. Pharmacological inhibition of p75 ^{NTR} or proNGF prevent elevation of TNFα and α_2M in DR. The levels of TNFα transcript were quantified by quantitative real-time PCR. ***A***, Retinas from 6 week diabetic mice $\pm$ treatment at week 2.5 of diabetes with anti-proNGF mAb, or THX-B, or vehicle, compared with age-matched naive control animals ($n = 3$/group). $^{**}p < 0.01$ (two-way ANOVA with significance $\alpha < 0.05$, followed by Bonferroni's correction). $^{***}p < 0.00$ (two-way ANOVA with significance $\alpha < 0.05$, followed by Bonferroni's correction). ***B***, rMC-1 glial cells were treated with varying concentrations of recombinant proNGF for 24 h, and TNFα mRNA levels were quantified. $^{*}p < 0.05$ (one-way ANOVA with significance $\alpha < 0.05$). $n = 6$. ***C***, rMC-1 cells treated with 1 ng/ml proNGF in the presence or absence of anti-proNGF mAb or p75 ^{NTR} inhibitor THX-B. Both treatments inhibited proNGF-induced TNFα mRNA increases. (*Figure legend continues.*)

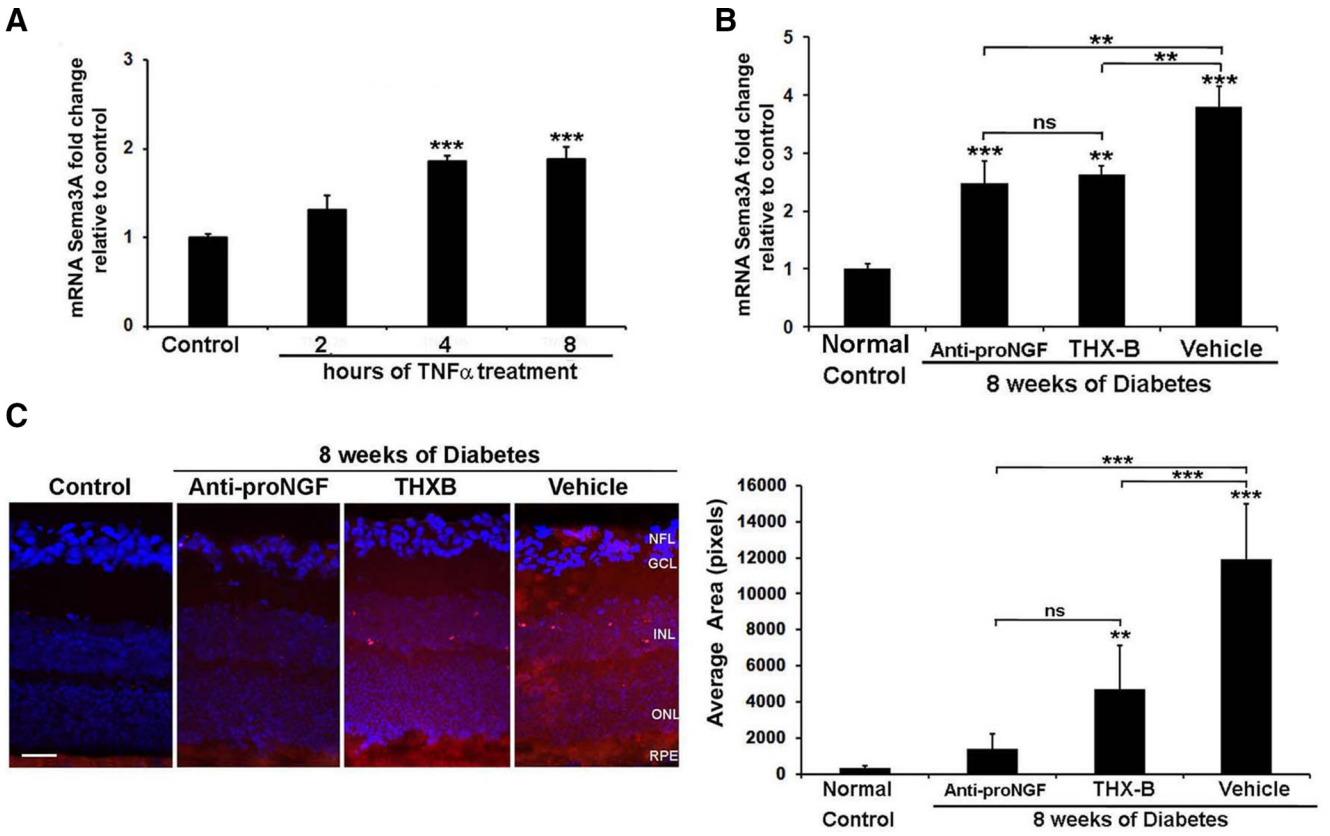

Figure 5. Inhibition of p75^{NTR} or proNGF efficiently reduces pathological vascular permeability in DR. Quantification of the levels of Sema3A transcript by qPCR on (***A***) Retinal neuronal cell line (RGC 5) treated for 2, 4, and 8 h with TNFα. Sema3A increased over time, compared with basal levels. ***$p < 0.001$ (one-way ANOVA with significance $\alpha < 0.05$). $n = 6$. ***B***, Retinas of 8 week diabetic mice ± treatment at week 2.5 of diabetes with anti-proNGF mAb or THX-B or vehicle, compared with age-matched naive control animals. Anti-proNGF mAb or THX-B significantly decreased Sema 3A mRNA compared with contralateral diabetic vehicle-treated retinas. **$p < 0.01$ (two-way ANOVA with significance $\alpha < 0.05$ followed by Bonferroni's correction for multiple comparisons). ***$p < 0.001$ (two-way ANOVA with significance $\alpha < 0.05$ followed by Bonferroni's correction for multiple comparisons). $n = 5$. ***C***, Confocal images of retinal sections from 6 week diabetic mice ± treatment at week 2.5 of diabetes with anti-proNGF mAb or THX-B or vehicle, compared with age-matched naive control animals. Red signal represents leakage of Evans blue dye from the vasculature into the retina. Images are representative of three independent experiments. Scale bar, 30 μm. Data were quantified using ImageJ as the average pixel area ± SD. **$p < 0.01$ (two-way ANOVA with significance $\alpha < 0.05$ followed by Bonferroni's correction for multiple comparisons). ***$p < 0.001$ (two-way ANOVA with significance $\alpha < 0.05$ followed by Bonferroni's correction for multiple comparisons). $n = 3$ independent experiments. ns, Not significant.

mRNA ($p < 0.01$) in THX-B-treated compared with vehicle-treated OIR pups (Fig. 6*C*,*D*). Given that TNFα can also affect vessel integrity, we asked whether proNGF/p75^{NTR}-mediated increases in TNFα affect endothelial cell survival. We treated RBMVECs with CM from proNGF-stimulated rMC-1 cells and measured cell survival. Media from proNGF-stimulated rMC-1 caused an ~70% reduction in survival ($p < 0.001$) compared with CM from vehicle-treated rMC-1. CM from rMC-1 cells treated with proNGF and either THX-B or anti-proNGF mAb did not promote the death of RBMVECs. As control, direct treatment of RBMVECs with proNGF had no effect on survival (Fig. 6*E*). Together, these results indicate that in OIR, as well as in diabetes, proNGF induces TNFα production in a p75^{NTR}-dependent manner, which may cause endothelial cell death and contribute to the VO.

←

(*Figure legend continued.*) **$p < 0.01$ (two-way ANOVA with significance $\alpha < 0.05$). ***$p < 0.001$ (two-way ANOVA with significance $\alpha < 0.05$). $n = 7$ or 8. Anti-proNGF mAb or THX-B in the absence of 1 ng/ml proNGF, as controls, had no effect. ***D***, p75^{NTR}, proNGF, TNFα, and α_2M expression in whole retina analyzed by Western blot of 6 week diabetic mice ± treatment at week 2.5 of diabetes with anti-proNGF mAb or THX-B or vehicle, compared with age-matched naive control animals. Both treatments significantly prevented the increased TNFα and α_2M, without affecting p75^{NTR} levels. As expected, the anti-proNGF mAb reduced the level of proNGF protein. Histograms show quantification relative to control or to the group indicated by each bracket. *$p < 0.05$ (two-way ANOVA with significance $\alpha < 0.05$, followed by Bonferroni's correction). **$p < 0.01$ (two-way ANOVA with significance $\alpha < 0.05$, followed by Bonferroni's correction). ***$p < 0.001$ (two-way ANOVA with significance $\alpha < 0.05$, followed by Bonferroni's correction). $n = 3$ independent experiments. ***E***, ***F***, Representative confocal microscopy images depicting the expression of TNFα and α_2M in retina sections of 6 week diabetic mice ± treatment with anti-proNGF mAb or THX-B or vehicle at week 2.5 of diabetes, compared with age-matched naive control animals. TNFα (green) was localized around the end-feet of CRALBP-positive (red) Müller cells around GCLs, whereas α_2M (green) showed a diffuse pattern of staining around vessels and surrounding the somata of cells in the GCL. The expression of both TNFα and α_2M was reduced on diabetic mice treated with anti-proNGF mAb or THX-B compared with vehicle-treated mice. Nuclei are counterstained with DAPI. Scale bar, 30 μm. NFL, Nerve fiber layer; RPE, retinal pigment epithelium; ns, not significant.

Pharmacological inhibition of p75^{NTR} diminishes pathological NV in OIR

We next characterized neurotrophic changes during the neovascular phase of OIR. Although there were no detectable changes in protein levels of proNGF or mature NGF in OIR compared with normoxia (data not shown), the protein levels of p75^{NTR} were significantly increased in OIR at P14 ($p < 0.01$) and P17 ($p < 0.001$) (Fig. 7*A*). Immunofluorescence of retinal sagittal sections from P17 OIR mice demonstrated a preferential increase of p75^{NTR} in glutamine synthetase-positive Müller cell end-feet and in GFAP^{+} cells in P17 OIR compared with normoxia (Fig. 7*B*). There was also an increase in p75^{NTR} in astrocytes surrounding lectin-positive vascular endothelial cells (Fig. 7*B*). These results

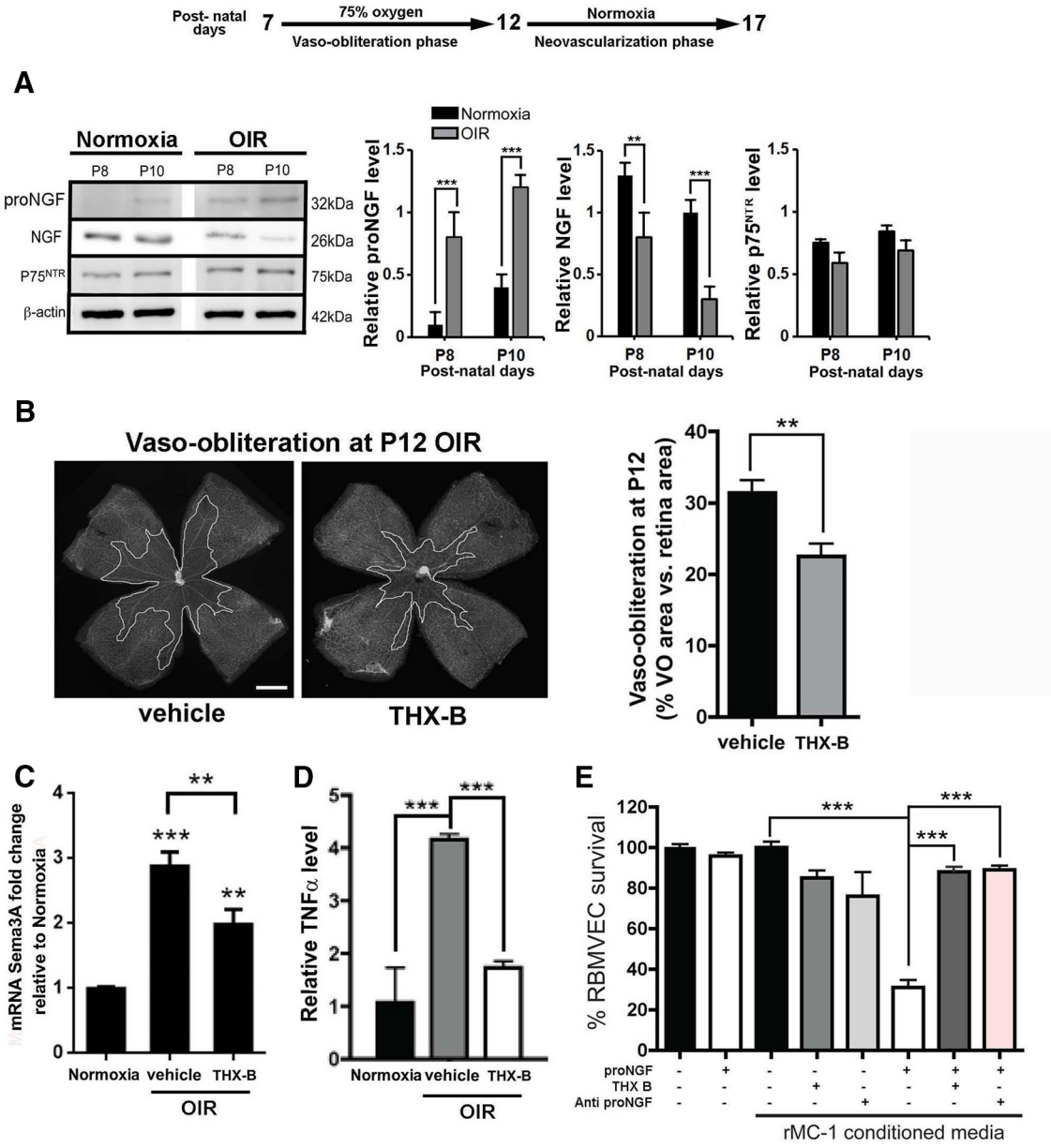

Figure 6. Inhibition of p75 ^{NTR} or proNGF reduces endothelial death during the VO phase of OIR. ***A***, proNGF, mature NGF, and p75 ^{NTR} expression in whole mice retina analyzed by Western blot in the VO phase of the OIR (P7-P12 at 75% O_2). ProNGF increased significantly during oxygen exposure relative to normoxia, whereas expression of mature NGF decreased significantly following oxygen exposure (mature NGF is a 26 kDa dimer in nonreduced SDS-PAGE). p75 ^{NTR} did not show significant changes. Quantification is shown on histogram. $^{**}p < 0.01$ (one-way ANOVA with significance $\alpha < 0.05$). $^{***}p < 0.001$ (one-way ANOVA with significance $\alpha < 0.05$). $n = 2$ independent experiments. ***B***, Representative photomicrographs from isolectin B4-stained retinal flat mounts from P12 mice pups exposed to hyperoxia from P7 to P12. Original magnification 100×. Pups injected intravitreally at P7 with THX-B had significantly less VO at P12 compared with vehicle-injected mice. $^{**}p < 0.01$ (two-tailed Student's *t* test). $n = 6$ –9 retinas. ***C***, The levels of Sema3A mRNA expression were quantified from real-time PCR of P9 whole retina of mice exposed or not to OIR, and injected at P7 with vehicle or THX-B. Mice injected with THX-B suppressed OIR-induced Sema3A mRNA expression. $^{**}p < 0.01$. $n = 4$. ***D***, The levels of TNFα mRNA expression were quantified from real-time PCR of P9 whole retina of mice exposed or not to OIR, and injected at P7 with vehicle or THX-B. Mice injected with THX-B suppressed OIR-induced TNFα mRNA expression. $^{***}p < 0.001$ (two-way ANOVA with significance $\alpha < 0.05$). $n = 4$. ***E***, RBMVEC metabolic/survival assay by MTT. Cultures exposed to CM from proNGF-stimulated rMC-1 cells had increased endothelial cell (EC) death. Addition of anti-proNGF mAb or p75 ^{NTR} inhibitor THX-B reduced proNGF-induced EC death. Controls using rMC-1 CM treated with inhibitors alone or ECs stimulated directly with proNGF had no effect. $^{***}p < 0.001$ (two-way ANOVA with significance $\alpha < 0.05$). $n = 6$.

indicate increased expression of glial p75 ^{NTR} during the neovascular phase of OIR and suggest a potential role in NV. Interestingly, these phenotypic results are similar to what we detected in diabetic mice.

To determine the contribution of p75 ^{NTR} to the phase of pathological angiogenesis in OIR, pups were injected intravitreally with THX-B at P12. Treatment with THX-B led to significantly reduced avascular area and to significantly reduced pathological NV at P17 compared with vehicle-injected mice ($p < 0.05$) (Fig. 7*C*). Interestingly, administration of THX-B at P14 had no effect on avascular area or on NV at P17, supporting the notion that p75 ^{NTR} activity is relevant during the early phases of NV.

THX-B inhibits VO during a period when VEGF levels are suppressed due to high oxygen tension (P7-P12). This suggests that p75 inhibitors act independent of VEGF. Normalization of Sema3A levels by THX-B treatment was significant in the vaso-obliterative phase. Because Sema3A deviates regenerating retinal vessels in the vasoproliferative phase (Cerani et al., 2013; Joyal et

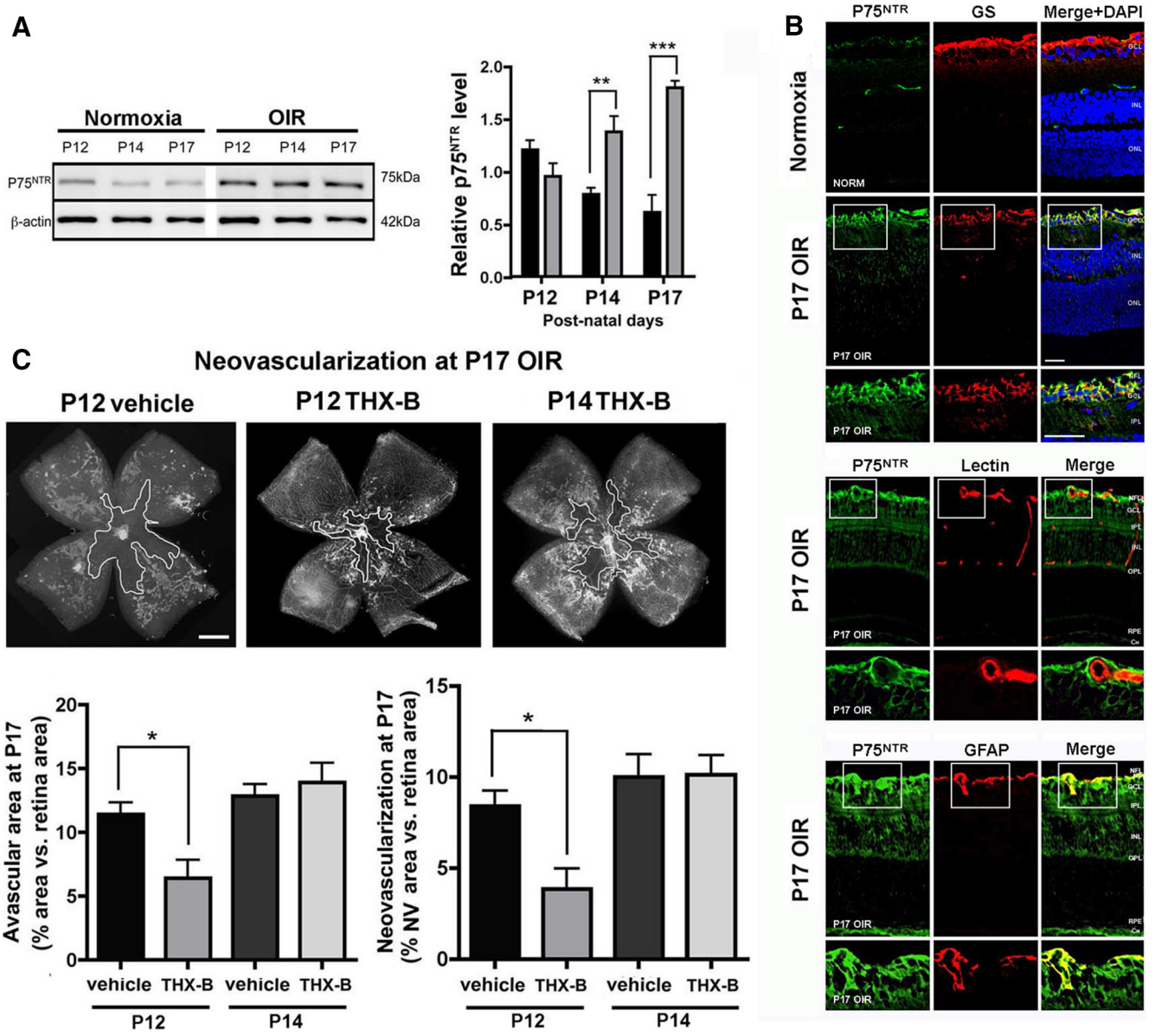

Figure 7. Inhibition of p75^{NTR} or proNGF reduces the NV area in OIR. ***A***, p75^{NTR} expression in whole retina analyzed by Western blot at three time points after OIR (P7-P12 at 75% O_2). Levels of p75^{NTR} increased significantly during this neovascular phase, relative to control normoxia retinas. Histogram represents quantification. One-way ANOVA with significance $\alpha < 0.05$: $^{**}p < 0.01$; $^{***}p < 0.001$. $n = 2$ independent experiments. ***B***, Distribution of p75^{NTR} in P17 retina exposed to OIR. p75^{NTR} (green) was found preferentially in glutamine synthetase (GS)-positive Müller cells (red), around the vessels labeled with Lectin (red) and GFAP-positive astrocytes (red). Nuclei are counterstained with DAPI. Top, Original magnification 300×. Scale bar, 50 μm. Bottom, Original magnification 600×. Scale bar, 30 μm. NFL, Nerve fiber layer. ***C***, Photomicrographs from isolectin B4-stained retinal flat mounts from P17 retinas from OIR mice injected intravitreally at P12 with THX-B demonstrated significantly less avascular area and less pathological NV compared with vehicle-treated mice. Late treatment using THX-B at P14 did not ameliorate revascularization. Scale bar, 100 μm. $^{*}p < 0.05$ (two-tailed Student's *t* test). $n = 4 – 6$ retinas.

al., 2013), p75 inhibitors lead to normalized angiogenesis and reduce destructive preretinal angiogenesis. Together, these results demonstrate that upregulation of proNGF and p75^{NTR} in Müller cells during the VO phase of OIR, and upregulation of p75^{NTR} in Müller cells and astrocytes in the NV phase of OIR can, respectively, promote vascular decay and pathological angiogenesis in part through TNFα and Sema3A.

Discussion

In humans, the pathophysiology of DR is characterized by a cascade of events, such as glial activation, inflammation, RGC death, capillary dropout, and loss of the BRB function causing retinal edema and ischemia. This ischemia leads to hypoxia and triggers a subsequent phase of neovascular DR (PDR). However, it is unknown whether these multiple pathophysiological events are sequential during disease progression and whether they are related mechanistically. While literature demonstrated the impact of glial activation and neuronal dysfunction in the pathogenesis of DR, and these often occur before measurable vascular abnormalities, the sequence of pathological events during disease progression remains unclear. Here, we demonstrate that prototypic Müller cell activation is propagated by p75^{NTR} in a proNGF-dependent manner early on at the onset of diabetes (week 1 and 2 following STZ). Moreover, we demonstrate that Müller cell activation increases local expression of TNFα and α_2M, which induce Sema3A in RGCs leading to BRB breakdown, heightened inflammation, and fluid extravasation into the retina. Fluid ex-

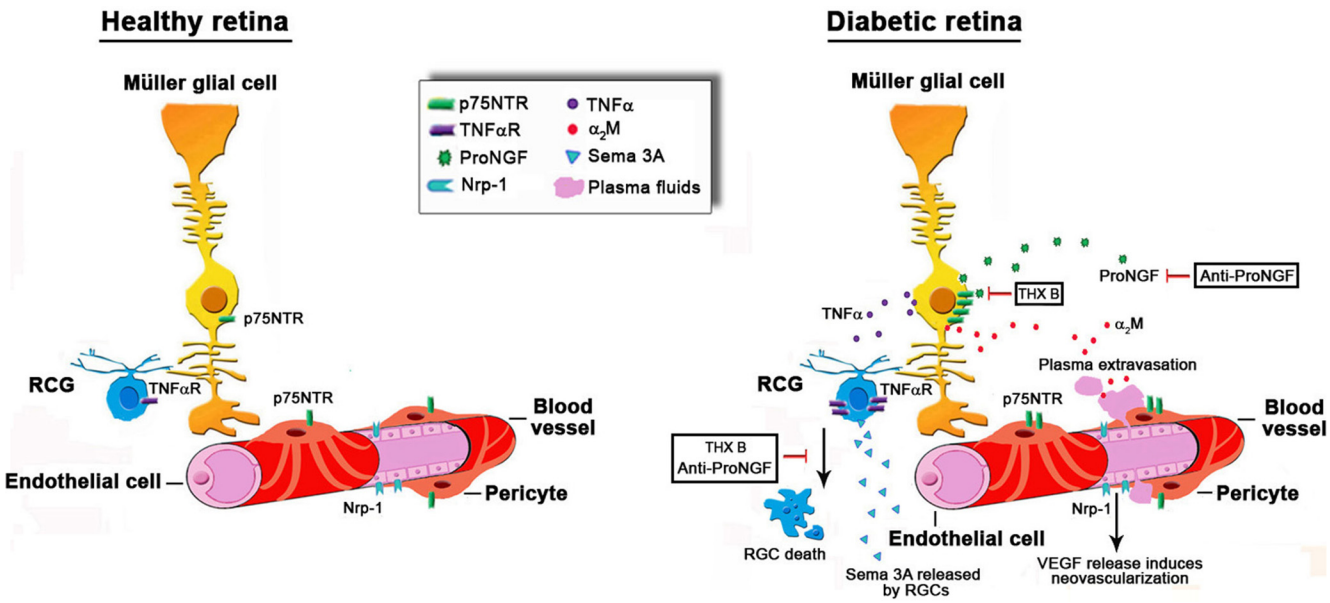

Figure 8. Model summarizing the etiology of p75^{NTR} in DR. In a healthy mature retina, the levels of p75^{NTR} are low. In diabetes, proNGF is significantly increased and activates p75^{NTR}, which is upregulated in Müller glial cells and pericytes. In Müller cells, p75^{NTR} activity triggers the expression/secretion of α_2M and TNFα. α_2M potentiates proNGF, thus creating a vicious cycle. Upregulated TNFα binds to receptors in RGCs inducing the release of Sema3A and eventual RGC death. Sema3A binds to its receptor Nrp1 and provokes loosening of endothelial cell junctions in the BRB and leads to plasma extravasation. In pericytes, p75^{NTR} activity could presumably trigger dysfunction and loss of vascular integrity, but this was not evaluated in this study. Intravitreal injections of THX-B or the anti-proNGF mAb in diabetic mice significantly diminished Müller glia activation, decreased TNFα and α_2M expression, limited Sema3A production, maintained BRB integrity, and prevented RGC neuronal cell death.

travasation brings in the retina additional toxic factors, such as α_2M, which exacerbate local inflammation.

The combination of all these events results in loss of retinal structure and irreversible RGC death leading to decreased visual acuity similar to that in patients with DR (Binet et al., 2013). This is in agreement with previous studies demonstrating that Sema3A is secreted by RGCs in response to the proinflammatory cytokine IL-1β, leading to the disruption of the vascular integrity in a model of proliferative retinopathy (Sitaras et al., 2015). Antagonizing p75^{NTR} with THX-B or administration of an inhibitory antibody to proNGF in mice with Type 1 DM, resulted in diminished Müller glia activation, curbed TNFα, α_2M and Sema3A expression, maintained BRB integrity, and prevented diabetes-induced neuronal cell and fiber loss.

With respect to NV, which occurs at a later stage of the disease, we describe important contributions of the p75^{NTR}/proNGF signaling axis. We describe, using a mouse model of OIR, ligand-dependent actions of p75^{NTR} on pathological preretinal neovessel formation, and demonstrate that proNGF and p75^{NTR} increase in mice exposed to OIR and stimulate production of TNFα in Müller cells. This paracrine mechanism can augment vascular decay and may contribute to pathological NV as previously reported (Gardiner et al., 2005; Stahl et al., 2010), events that are reminiscent of DR.

Our data not only corroborate previous studies demonstrating the pathogenic effects of increased TNFα (Gardiner et al., 2005; Le Moan et al., 2011) and Sema3A (Gardiner et al., 2005) during the phase of NV but demonstrates a potential regulation by p75^{NTR} signaling. Both the VO as well as the resulting NV can be ameliorated by antagonizing p75^{NTR} or proNGF. Together, these studies validate a novel mechanism of action and provide evidence of a novel druggable therapeutic target that can ameliorate several of the pathological components of DR.

In the DR model, the p75/proNGF axis is upregulated before any measurable retinal damage, and before upregulation of retinal TNFα and α2M mRNA and protein, cytokines that are thought to contribute to the DR pathology. In that sense, p75/proNGF appears to be upstream of these inflammatory mediators. Inhibition of p75/proNGF reduces the inflammatory mediators and improves retinal health. Improved retinal health may then contribute to the long-term reduction in inflammatory mediators in DR. A similar conclusion would be germane in the OIR model, where the p75/proNGF axis is upregulated before TNFα and Sema3A, and inhibition of p75/proNGF reduces the mediators and improves retinal health.

Although the therapeutic effect of either p75^{NTR} or proNGF antagonists was generally comparable, discrepancies were observed likely due to ligand-independent actions of p75^{NTR}. For instance, although expression of proNGF did not seem to increase during the second phase of OIR (compared with control room-air raised animals), inhibition of p75^{NTR} activity via THX-B antagonism successfully curbed pathological angiogenesis and promoted normal revascularization. Of note, there is evidence for ligand-independent actions of p75^{NTR} in pathological NV in the mouse model of OIR whereby the γ-secretase-mediated cleavage of the intracellular domain of p75^{NTR} enhances interaction with Siah2 (which prevents HIF-1α degradation) in Müller cells, and increases VEGF expression in the retina. (Le Moan et al., 2011). Thus, antagonizing p75^{NTR} with THX-B may prevent cleavage of the p75^{NTR} intracellular domain permitting Siah2-mediated degradation of HIF-1α, which diminishes VEGF expression and pathological neovessel formation.

The important role of retinal microglia as responder to retinal injuries has been described previously (Cuenca et al., 2014; Karlstetter et al., 2015). In the STZ model in rats, microglia are found in retina after 4 weeks of diabetes, and microglia activation leads to the release of TNFα and IL-1, which contributes to vascular and neuronal cell death (Krady et al., 2005). However, these microglia events take place after the p75/proNGF axis reported herein, which largely involve Müller cells as a first step. We speculate that it is possible that, by inhibiting the p75/proNGF axis, microglia activation may thus also be prevented, due to an overall improved retinal health.

The data support a model (Fig. 8) explaining the mechanisms by which $p75^{NTR}$ mediates different phases of the DR. The early and persistent upregulation of $p75^{NTR}$, mainly in Müller glial cells, plays a pivotal role in disrupting neuro-glia-vascular unit in the DR. More specifically, p75NTR signaling promotes, in a ligand-dependent manner, production of the inflammatory cytokines TNFα and α_2M and Sema3A, leading to RGC death, BRB breakdown, and edema. Similarly, $p75^{NTR}$ activity contributes to retinal VO and NV via increased TNFα and Sema3A production. To illustrate this phenomenon, we propose a hypothetical model to integrate these observations (Fig. 8). In DR, resident Müller glia undergo activation and gliosis augmenting the production of $p75^{NTR}$. Activated Müller cells rapidly increase the levels of proNGF, and autocrine binding of proNGF to $p75^{NTR}$ promotes the production and release of proinflammatory cytokines, such as TNFα and α_2M. TNFα and α_2M act via two different paracrine mechanisms. First, TNFα binds to its receptor on RGCs and prompts the secretion of the vascular cue Sema3A. Excessive accumulation of TNFα and α_2M ultimately causes RGC death and the secretion of Sema3A from RGCs, which influence endothelial cells by binding, most likely, to its receptor Neuropilin-1 (Cerani et al., 2013). Sema3A causes early BRB breakdown and plasma extravasation. Ligand-dependent production of inflammatory cytokines, RGC death, BRB breakdown, and edema were significantly decreased by treatment with anti-proNGF mAb or the $p75^{NTR}$ antagonist THX-B. Second, TNFα acts directly on endothelial cells inducing cell death, which contribute to vessel loss during the first phase of the vascular component of the disease. Both anti-proNGF mAb and THX-B treatments also reduced pathological NV. In conclusion, $p75^{NTR}$ and proNGF are key mediators at different stages of the DR. These antagonists may be novel therapeutic targets that offer a wide range spectrum of action and an alternative approach to the VEGF-based strategy.

In conclusion, our data identify a novel mechanism implicating neuronal, glial, and vascular interplay in the pathogenesis of DR. In doing so, we provide evidence for p75 as a promising therapeutic target to counter several stages of DR.

References

Abcouwer SF, Gardner TW (2014) Diabetic retinopathy: loss of neuroretinal adaptation to the diabetic metabolic environment. Ann N Y Acad Sci 1311:174–190. CrossRef Medline

Al-Gayyar MM, Matragoon S, Pillai BA, Ali TK, Abdelsaid MA, El-Remessy AB (2011) Epicatechin blocks pro-nerve growth factor (proNGF)-mediated retinal neurodegeneration via inhibition of p75 neurotrophin receptor expression in a rat model of diabetes [corrected]. Diabetologia 54:669–680. CrossRef Medline

Ali TK, Matragoon S, Pillai BA, Liou GI, El-Remessy AB (2008) Peroxynitrite mediates retinal neurodegeneration by inhibiting nerve growth factor survival signaling in experimental and human diabetes. Diabetes 57:889–898. CrossRef Medline

Antonetti DA, Klein R, Gardner TW (2012) Diabetic retinopathy. N Engl J Med 366:1227–1239. CrossRef Medline

Bai Y, Dergham P, Nedev H, Xu J, Galan A, Rivera JC, ZhiHua S, Mehta HM, Woo SB, Sarunic MV, Neet KE, Saragovi HU (2010a) Chronic and acute models of retinal neurodegeneration TrkA activity are neuroprotective whereas p75NTR activity is neurotoxic through a paracrine mechanism. J Biol Chem 285:39392–39400. CrossRef Medline

Bai Y, Shi Z, Zhuo Y, Liu J, Malakhov A, Ko E, Burgess K, Schaefer H, Esteban PF, Tessarollo L, Saragovi HU (2010b) In glaucoma the up-regulated truncated TrkC.T1 receptor isoform in glia causes increased TNF-α production, leading to retinal ganglion cell death. Invest Ophthalmol Vis Sci 51:6639–6651. CrossRef Medline

Bai Y, Sivori D, Woo SB, Neet KE, Lerner SF, Saragovi HU (2011) During glaucoma, alpha2-macroglobulin accumulates in aqueous humor and binds to nerve growth factor, neutralizing neuroprotection. Invest Ophthalmol Vis Sci 52:5260–5265. CrossRef Medline

Barcelona PF, Saragovi HU (2015) A pro-nerve growth factor (proNGF) and NGF binding protein, alpha2-macroglobulin, differentially regulates p75 and TrkA receptors and is relevant to neurodegeneration ex vivo and in vivo. Mol Cell Biol 35:3396–3408. CrossRef Medline

Binet F, Mawambo G, Sitaras N, Tetreault N, Lapalme E, Favret S, Cerani A, Leboeuf D, Tremblay S, Rezende F, Juan AM, Stahl A, Joyal JS, Milot E, Kaufman RJ, Guimond M, Kennedy TE, Sapieha P (2013) Neuronal ER stress impedes myeloid-cell-induced vascular regeneration through IRE1alpha degradation of netrin-1. Cell Metab 17:353–371. CrossRef Medline

Bringmann A, Pannicke T, Grosche J, Francke M, Wiedemann P, Skatchkov SN, Osborne NN, Reichenbach A (2006) Müller cells in the healthy and diseased retina. Prog Retin Eye Res 25:397–424. CrossRef Medline

Cerani A, Tetreault N, Menard C, Lapalme E, Patel C, Sitaras N, Beaudoin F, Leboeuf D, De Guire V, Binet F, Dejda A, Rezende FA, Miloudi K, Sapieha P (2013) Neuron-derived semaphorin 3A is an early inducer of vascular permeability in diabetic retinopathy via neuropilin-1. Cell Metab 18:505–518. CrossRef Medline

Coorey NJ, Shen W, Chung SH, Zhu L, Gillies MC (2012) The role of glia in retinal vascular disease. Clin Exp Optom 95:266–281. CrossRef Medline

Cuenca N, Fernández-Sánchez L, Campello L, Maneu V, De la Villa P, Lax P, Pinilla I (2014) Cellular responses following retinal injuries and therapeutic approaches for neurodegenerative diseases. Prog Retin Eye Res 43:17–75. CrossRef Medline

Dejda A, Mawambo G, Cerani A, Miloudi K, Shao Z, Daudelin JF, Boulet S, Oubaha M, Beaudoin F, Akla N, Henriques S, Menard C, Stahl A, Delisle JS, Rezende FA, Labrecque N, Sapieha P (2014) Neuropilin-1 mediates myeloid cell chemoattraction and influences retinal neuroimmune crosstalk. J Clin Invest 124:4807–4822. CrossRef Medline

Esquiva G, Lax P, Cuenca N (2013) Impairment of intrinsically photosensitive retinal ganglion cells associated with late stages of retinal degeneration. Invest Ophthalmol Vis Sci 54:4605–4618. CrossRef Medline

Fletcher EL, Phipps JA, Ward MM, Puthussery T, Wilkinson-Berka JL (2007) Neuronal and glial cell abnormality as predictors of progression of diabetic retinopathy. Curr Pharm Des 13:2699–2712. CrossRef Medline

Frade JM, Bovolenta P, Rodríguez-Tébar A (1999) Neurotrophins and other growth factors in the generation of retinal neurons. Microsc Res Tech 45:243–251. CrossRef Medline

García-Ayuso D, Salinas-Navarro M, Agudo M, Cuenca N, Pinilla I, Vidal-Sanz M, Villegas-Pérez MP (2010) Retinal ganglion cell numbers and delayed retinal ganglion cell death in the P23H rat retina. Exp Eye Res 91:800–810. CrossRef Medline

García-Ayuso D, Di Pierdomenico J, Esquiva G, Nadal-Nicolás FM, Pinilla I, Cuenca N, Vidal-Sanz M, Agudo-Barriuso M, Villegas-Pérez MP (2015) Inherited photoreceptor degeneration causes the death of melanopsin-positive retinal ganglion cells and increases their coexpression of Brn3a. Invest Ophthalmol Vis Sci 56:4592–4604. CrossRef Medline

Gardiner TA, Gibson DS, de Gooyer TE, de la Cruz VF, McDonald DM, Stitt AW (2005) Inhibition of tumor necrosis factor-alpha improves physiological angiogenesis and reduces pathological neovascularization in ischemic retinopathy. Am J Pathol 166:637–644. CrossRef Medline

Heng LZ, Comyn O, Peto T, Tadros C, Ng E, Sivaprasad S, Hykin PG (2013) Diabetic retinopathy: pathogenesis, clinical grading, management and future developments. Diabet Med 30:640–650. CrossRef Medline

Jian Y, Wong K, Sarunic MV (2013) Graphics processing unit accelerated optical coherence tomography processing at megahertz axial scan rate and high resolution video rate volumetric rendering. J Biomed Opt 18:26002. CrossRef Medline

Joyal JS, Sitaras N, Binet F, Rivera JC, Stahl A, Zaniolo K, Shao Z, Polosa A, Zhu T, Hamel D, Djavari M, Kunik D, Honoré JC, Picard E, Zabeida A, Varma DR, Hickson G, Mancini J, Klagsbrun M, Costantino S, et al. (2013) Ischemic neurons prevent vascular regeneration of neural tissue by secreting semaphorin 3A. Blood 117:6024–6035. CrossRef Medline

Karlstetter M, Scholz R, Rutar M, Wong WT, Provis JM, Langmann T (2015) Retinal microglia: just bystander or target for therapy? Prog Retin Eye Res 45:30–57. CrossRef Medline

Kowluru RA, Chan PS (2007) Oxidative stress and diabetic retinopathy. Exp Diabetes Res 2007:43603. CrossRef Medline

Krady JK, Basu A, Allen CM, Xu Y, LaNoue KF, Gardner TW, Levison SW (2005) Minocycline reduces proinflammatory cytokine expression, microglial activation, and caspase-3 activation in a rodent model of diabetic retinopathy. Diabetes 54:1559–1565. CrossRef Medline

Lebrun-Julien F, Duplan L, Pernet V, Osswald I, Sapieha P, Bourgeois P, Dickson K, Bowie D, Barker PA, Di Polo A (2009a) Excitotoxic death of retinal neurons in vivo occurs via a non-cell-autonomous mechanism. J Neurosci 29:5536–5545. CrossRef Medline

Lebrun-Julien F, Morquette B, Douillette A, Saragovi HU, Di Polo A (2009b) Inhibition of p75(NTR) in glia potentiates TrkA-mediated survival of injured retinal ganglion cells. Mol Cell Neurosci 40:410–420. CrossRef Medline

Lebrun-Julien F, Bertrand MJ, De Backer O, Stellwagen D, Morales CR, Di Polo A, Barker PA (2010) ProNGF induces TNFalpha-dependent death of retinal ganglion cells through a p75NTR non-cell-autonomous signaling pathway. Proc Natl Acad Sci U S A 107:3817–3822. CrossRef Medline

Le Moan N, Houslay DM, Christian F, Houslay MD, Akassoglou K (2011) Oxygen-dependent cleavage of the p75 neurotrophin receptor triggers stabilization of HIF-1alpha. Mol Cell 44:476–490. CrossRef Medline

Li J, Bloch P, Xu J, Sarunic MV, Shannon L (2011) Performance and scalability of Fourier domain optical coherence tomography acceleration using graphics processing units. Appl Opt 50:1832–1838. CrossRef Medline

Ma N, Hunt NH, Madigan MC, Chan-Ling T (1996) Correlation between enhanced vascular permeability, up-regulation of cellular adhesion molecules and monocyte adhesion to the endothelium in the retina during the development of fatal murine cerebral malaria. Am J Pathol 149: 1745–1762. Medline

Mysona BA, Al-Gayyar MM, Matragoon S, Abdelsaid MA, El-Azab MF, Saragovi HU, El-Remessy AB (2013) Modulation of p75(NTR) prevents diabetes- and proNGF-induced retinal inflammation and blood–retina barrier breakdown in mice and rats. Diabetologia 56:2329–2339. CrossRef Medline

Saragovi HU, Zheng W, Maliartchouk S, DiGugliemo GM, Mawal YR, Kamen A, Woo SB, Cuello AC, Debeir T, Neet KE (1998) A TrkA-selective, fast internalizing nerve growth factor-antibody complex induces trophic but not neuritogenic signals. J Biol Chem 273:34933–34940. CrossRef Medline

Sarunic MV, Yazdanpanah A, Gibson E, Xu J, Bai Y, Lee S, Saragovi HU, Beg MF (2010) Longitudinal study of retinal degeneration in a rat using spectral domain optical coherence tomography. Opt Express 18:23435–23441. CrossRef Medline

Shi Z, Rudzinski M, Meerovitch K, Lebrun-Julien F, Birman E, Di Polo A, Saragovi HU (2008) Alpha2-macroglobulin is a mediator of retinal ganglion cell death in glaucoma. J Biol Chem 283:29156–29165. CrossRef Medline

Siao CJ, Lorentz CU, Kermani P, Marinic T, Carter J, McGrath K, Padow VA, Mark W, Falcone DJ, Cohen-Gould L, Parrish DC, Habecker BA, Nykjaer A, Ellenson LH, Tessarollo L, Hempstead BL (2012) ProNGF, a cytokine induced after myocardial infarction in humans, targets pericytes to promote microvascular damage and activation. J Exp Med 209:2291–2305. CrossRef Medline

Sitaras N, Rivera JC, Noueihed B, Bien-Aime M, Zaniolo K, Omri S, Hamel D, Zhu T, Hardy P, Sapieha P, Joyal JS, Chemtob S (2015) Retinal neurons curb inflammation and enhance revascularization in ischemic retinopathies via proteinase-activated receptor-2. J Pathol 185:581–595. CrossRef Medline

Smith LE, Wesolowski E, McLellan A, Kostyk SK, D'Amato R, Sullivan R, D'Amore PA (1994) Oxygen-induced retinopathy in the mouse. Invest Ophthalmol Vis Sci 35:101–111. Medline

Stahl A, Connor KM, Sapieha P, Willett KL, Krah NM, Dennison RJ, Chen J, Guerin KI, Smith LE (2009) Computer-aided quantification of retinal neovascularization. Angiogenesis 12:297–301. CrossRef Medline

Stahl A, Connor KM, Sapieha P, Chen J, Dennison RJ, Krah NM, Seaward MR, Willett KL, Aderman CM, Guerin KI, Hua J, Löfqvist C, Hellström A, Smith LE (2010) The mouse retina as an angiogenesis model. Invest Ophthalmol Vis Sci 51:2813–2826. CrossRef Medline

Yau JW, Rogers SL, Kawasaki R, Lamoureux EL, Kowalski JW, Bek T, Chen SJ, Dekker JM, Fletcher A, Grauslund J, Haffner S, Hamman RF, Ikram MK, Kayama T, Klein BE, Klein R, Krishnaiah S, Mayurasakorn K, O'Hare JP, Orchard TJ, et al. (2012) Global prevalence and major risk factors of diabetic retinopathy. Diabetes Care 35:556–564. CrossRef Medline